Sec1p and Mso1p C-terminal tails cooperate with the SNAREs and Sec4p in polarized exocytosis

Marion Weber-Boyvat[a], Nina Aro[a], Konstantin G. Chernov[a], Tuula Nyman[b], and Jussi Jäntti[a]
[a]Cell and Molecular Biology Program and [b]Research Program in Structural Biology and Biophysics, Institute of Biotechnology, FI-0001 University of Helsinki, Finland

ABSTRACT **The Sec1/Munc18 protein family members perform an essential, albeit poorly understood, function in association with soluble n-ethylmaleimide sensitive factor adaptor protein receptor (SNARE) complexes in membrane fusion. The *Saccharomyces cerevisiae* Sec1p has a C-terminal tail that is missing in its mammalian homologues. Here we show that deletion of the Sec1p tail (amino acids 658–724) renders cells temperature sensitive for growth, reduces sporulation efficiency, causes a secretion defect, and abolishes Sec1p-SNARE component coimmunoprecipitation. The results show that the Sec1p tail binds preferentially ternary Sso1p-Sec9p-Snc2p complexes and it enhances ternary SNARE complex formation in vitro. The bimolecular fluorescence complementation (BiFC) assay results suggest that, in the SNARE-deficient *sso2–1 Δsso1* cells, Mso1p, a Sec1p binding protein, helps to target Sec1p(1–657) lacking the C-terminal tail to the sites of secretion. The results suggest that the Mso1p C terminus is important for Sec1p(1–657) targeting. We show that, in addition to Sec1p, Mso1p can bind the Rab-GTPase Sec4p in vitro. The BiFC results suggest that Mso1p acts in close association with Sec4p on intracellular membranes in the bud. This association depends on the Sec4p guanine nucleotide exchange factor Sec2p. Our results reveal a novel binding mode between the Sec1p C-terminal tail and the SNARE complex, and suggest a role for Mso1p as an effector of Sec4p.**

Monitoring Editor
Patrick Brennwald
University of North Carolina

Received: Jul 13, 2010
Revised: Nov 3, 2010
Accepted: Nov 9, 2010

INTRODUCTION

Exocytosis involves transport vesicle targeting, tethering, and fusion at the plasma membrane. In the yeast *Saccharomyces cerevisiae*, this process is mediated by the exocyst complex (Guo *et al.*, 2000), the Rab family small guanosine triphosphatase (GTPase) Sec4p, the Sec1/Munc-18 (SM) family protein Sec1p (Novick and Guo, 2002; Toonen and Verhage, 2007; He and Guo, 2009), the Sec1p binding protein Mso1p (Knop *et al.*, 2005; Weber *et al.*, 2010), and the exocytic soluble n-ethylmaleimide sensitive factor adaptor protein receptor (SNARE) complex composed of Snc1p/2p, Sec9p, and Sso1p/2p proteins (Jahn and Scheller, 2006).

The SM protein family members are evolutionarily conserved proteins that perform an essential, albeit poorly understood, function in SNARE complex regulation in membrane fusion. *S. cerevisiae* Sec1p is a homologue of the mammalian Munc18–1 protein that binds syntaxin 1 and regulates syntaxin 1-synaptobrevin-SNAP-25 SNARE complex assembly (Toonen and Verhage, 2003). Munc18–1-syntaxin 1 association has been proposed to maintain syntaxin 1 in a closed conformation and to inhibit the syntaxin to enter the SNARE complex (Misura *et al.*, 2000). Sly1p, a SM protein involved in endoplasmic reticulum (ER)-to-Golgi trafficking, possesses a different binding mode in its interaction with the syntaxin homologue Sed5p. It has been shown to bind to the N-terminal peptide of Sed5p via its SNARE N-peptide binding site. This binding allows Sed5p to be in an open conformation with Sly1p attached to it (Bracher and Weissenhorn, 2002; Yamaguchi *et al.*, 2002; Arac *et al.*, 2005). In addition to the just described interaction modes, SM-family proteins (e.g., Sec1p) can interact with assembled ternary SNARE complexes (Carr *et al.*, 1999; Scott *et al.*, 2004; Togneri *et al.*, 2006). Recently it was shown that Munc18–1 binds with different affinities to the sole syntaxin 1, synaptobrevin, and the SNARE complexes using the different binding modes just described (Xu *et al.*, 2010). Despite these advances,

This article was published online ahead of print in MBoC in Press (http://www.molbiolcell.org/cgi/doi/10.1091/mbc.E10-07-0592) on November 30, 2010.

Address correspondence to: Jussi Jäntti (jussi.jantti@helsinki.fi).

Abbreviations used: BiFC, bimolecular fluorescence complementation; ER, endoplasmic reticulum; GAP, GTPase activating protein; GDP, guanosine diphosphate; GEF, guanine nucleotide exchange factor; GTP, guanosine triphosphate; GTPase, guanosine triphosphatase; PI(4)P, phosphatidylinositol-4-phosphate; SM, Sec1/Munc18; SNARE, soluble n-ethylmaleimide sensitive factor adaptor protein receptor.

there is a lack of detailed understanding of SM protein regulation and its function in membrane fusion.

Rab-family small guanosine triphosphate (GTP)-binding proteins act as upstream regulators of SNARE-mediated membrane fusion (Jahn and Scheller, 2006). In exocytosis, the Rab Sec4p is needed for SNARE complex formation and fusion of vesicles with the plasma membrane. The guanine nucleotide–binding state of Sec4p is regulated by several proteins, including the guanine nucleotide exchange factor (GEF) Sec2p (Walch-Solimena *et al.*, 1997); the GTPase activating proteins (GAPs) Gyl1p (Tarassov *et al.*, 2008), Gyp1p (Du *et al.*, 1998), Mdr1p (Albert and Gallwitz, 1999), and Msb4p (Albert and Gallwitz, 2000); and the guanine nucleotide dissociation stimulator Dss4p (Collins *et al.*, 1997). Recently it was shown that Sec2p displays a set of sequential protein–protein interactions with Ypt32p and Sec4p that are regulated by Sec2p binding to phosphatidylinositol-4-phosphate [PI(4)P] (Mizuno-Yamasaki *et al.*, 2010). These interactions are necessary for Sec2p membrane recruitment and transport vesicle maturation for downstream docking and fusion (Mizuno-Yamasaki *et al.*, 2010). It has been proposed that GTP-loaded Sec4p is bound to the secretory vesicle and that GTP hydrolysis is required for its downstream signal transmission (Walworth *et al.*, 1992; Armstrong, 2000). We have shown that deletion of the Sec1p binding protein Mso1p results in synthetic lethality when combined with mutations in Sec2p or Sec4p (Aalto *et al.*, 1997; Knop *et al.*, 2005). These synthetic interactions appear to be mediated by the carboxy-terminal part of Mso1p that is not needed for binding with Sec1p (Knop *et al.*, 2005). Furthermore, the association of the Mso1p-Sec1p complex with SNARE complexes is abolished in Sec4p-defective cells (Knop *et al.*, 2005; Weber *et al.*, 2010). These results indicate close interactions between Sec4p, Sec1p, and Mso1p in the regulation of *S. cerevisiae* exocytic SNARE complex function.

The exocyst complex, Sec4p, Sec1p, and SNARE complexes are well-established components required for exocytosis. It is poorly understood, however, how they cooperate to ensure correct docking and fusion of transport vesicles at the plasma membrane. The *S. cerevisiae* Sec1p has a 67-amino-acid-long C-terminal tail that is missing in its mammalian homologues. This C-terminal tail does not possess any obvious sequence motifs that would reveal its functional role in vivo. Here we show that the Sec1p C-terminal tail is important for Sec1p-SNARE complex interactions. Our results imply that the Sec1p binding protein Mso1p can target the SNARE binding deficient Sec1(1–657)p to sites of polarized membrane transport and that this function is mediated by the Mso1p C terminus. We show that Mso1p can interact with Sec4p in vitro and that the Mso1p C terminus functionally collaborates with the GTP-bound form of Sec4p prior to membrane fusion on vesicle-like structures close to the plasma membrane. This interaction is dependent on the Sec4p GEF Sec2p and independent of a functional SNARE complex. Our results reveal a close cooperation of the Sec1p C-terminal tail, Mso1p, and Sec4p in SNARE complex assembly.

RESULTS

Yeast Sec1p has a nonconserved C-terminal tail

SM protein family members are conserved regulators of SNARE complex function (Gallwitz and Jahn, 2003; Kauppi *et al.*, 2004; Toonen and Verhage, 2007). Comparison of the known SM protein structures shows that they possess a conserved arch-like structure (Gallwitz and Jahn, 2003; Toonen and Verhage, 2007). Upon sequence alignment of *S. cerevisiae* Sec1p with mouse Munc18–1 or fungal Sec1p homologues, it is evident that the fungal Sec1p homologues typically possess an additional C-terminal extension not present in higher eukaryotes (Figure 1A). This tail is conserved within different *Saccharomyces* species but is variable between other fungi (Figure 1A). Secondary structure prediction of the different fungal tail peptides revealed that they share a similar pattern and number of potential α-helixes (Figure 1B). Of the other *S. cerevisiae* SM family proteins Vps45p, Sly1p, and Vps33p, Vps45p and Sly1p do not possess a C-terminal extension with a similar predicted α-helical structure (Supplemental Figure S1). Vps33p has an approximately 30-amino-acid-long C-terminal tail, however. The most obvious feature of the *S. cerevisiae* Sec1p tail sequence is the high occurrence of basic, positively charged amino acids (23%). In Sec1p or its homologues, a cluster of basic amino acids is typically located at the C terminus of the tail. This feature is well conserved in *Schizosaccharomyces pombe* and *Neurospora crassa* Sec1p (Figure 1A, black shading).

The Sec1p tail is important for Sec1p in vivo function

Considering the fact that the C-terminal tail is conserved in the fungal Sec1p homologues, we wanted to evaluate its role for *S. cerevisiae* Sec1p function. For this, strains were generated in which the last 67 amino acids of Sec1p were deleted by the addition of a premature stop codon at the genomic *SEC1* locus. The generated Sec1p(1–657) lacks the C-terminal tail, thereby resembling the mouse Munc18–1 (Figure 1A).

Both haploid and homozygous diploid *sec1(1–657)* mutant cells were viable at 30°C. The haploid *sec1(1–657) MSO1-HA* strain, however, was mildly cold sensitive and clearly heat sensitive for growth (Figure 1C). At the same time, no temperature sensitivity was detected for the *SEC1* (wild type [wt]) *MSO1-HA* strain. In the homozygous *sec1(1–657)/sec1(1–657)* diploid cells, a 60% reduction in their ability to sporulate was observed (Figure 1D). This finding suggests that Sec1p(1–657) is functionally compromised in membrane fusion regulation during prospore membrane formation. When secretion of Bgl2p and Hsp150 was examined, intracellular accumulation of Bgl2p was evident already at 30°C. When the *sec1(1–657) MSO1-HA* cells were shifted to 37°C (Figure 1E), enhanced intracellular accumulation of Bgl2p was observed. At the same time, in *MSO1-HA* cells no accumulation of Bgl2p was observed. Interestingly, under identical experimental conditions no obvious defect in Hsp150 secretion was observed in *sec1(1–657) MSO1-HA* cells (Supplemental Figure S2).

The Sec1p tail is important for Sec1p interaction with SNARE complex components

The Sec1p(1–657) and wt Sec1p are expressed at similar levels (Figure 2A, input) indicating that the observed temperature sensitivity or Bgl2p secretion defect in *sec1(1–657)* cells is not due to reduced levels of the mutant protein. At the same time, expression of the Sec1p(1–657) as the sole copy of Sec1p in cells did not affect the expression levels of Sec9p, Sso1/2p, or Snc1/2p (Figure 2A, input). To understand the reason for the *sec1(1–657)* cell in vivo phenotype, immunoprecipitations were performed. It has been previously shown that Mso1p coimmunoprecipitates with Sec1p and SNARE components Sso1/2p-Sec9p-Snc1/2p (Castillo-Flores *et al.*, 2005; Knop *et al.*, 2005; Weber *et al.*, 2010). To assess the contribution of the Sec1p C-terminal tail for Mso1p and SNARE interactions, Mso1p-HA (expressed at the *MSO1* locus from its endogenous promoter) was immunoprecipitated with anti-HA antibodies and the coimmunoprecipitation of Sec1p and SNARE components was analyzed by SDS–PAGE and Western blotting. Compared to the wt Sec1p, there was no notable difference in the efficiency of Sec1p(1–657) coprecipitation with Mso1p (Figure 2A). At the same

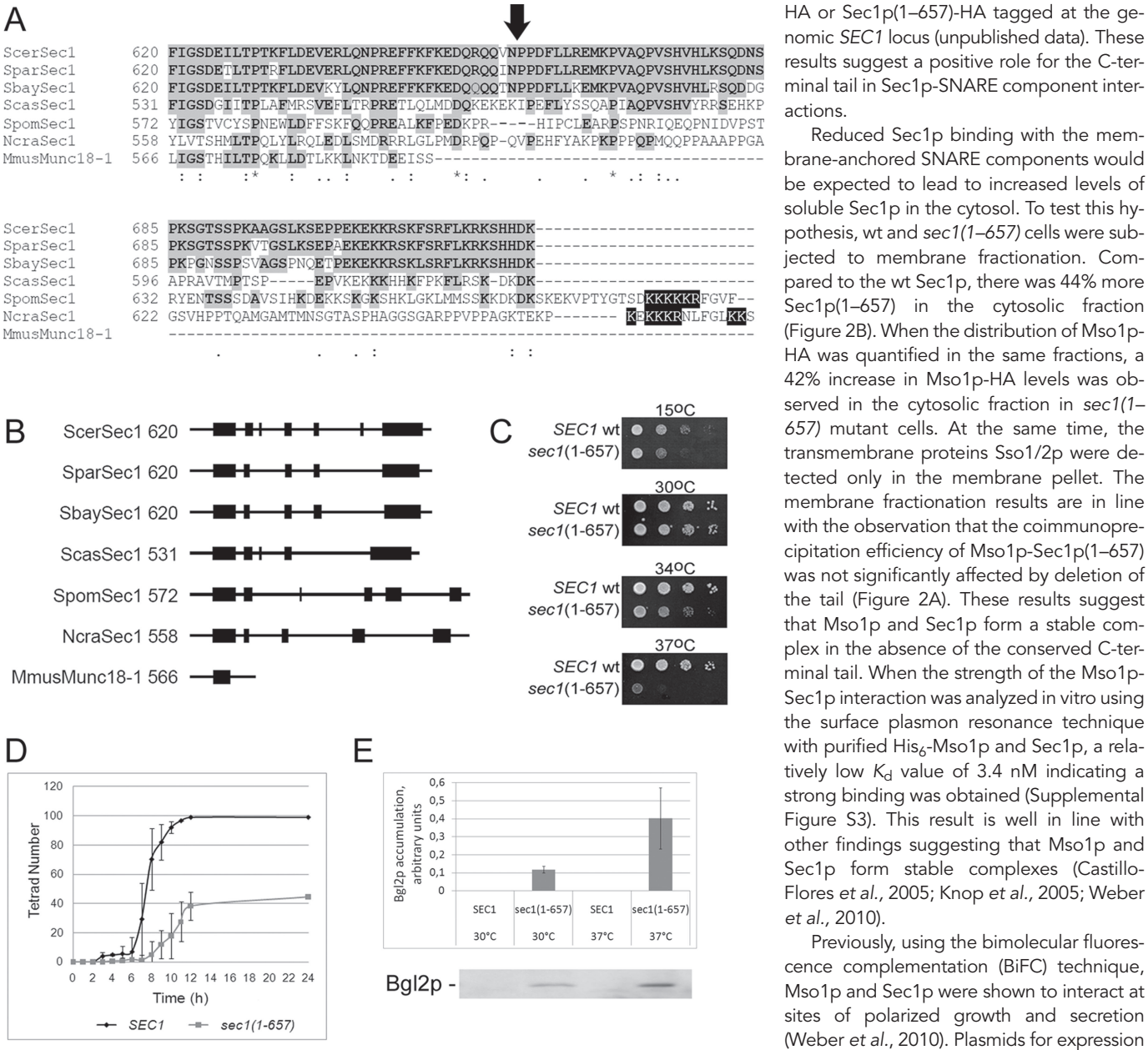

FIGURE 1: The C-terminal tail is important for *S. cerevisiae* Sec1p in vivo function. (A) Comparison of *S. cerevisiae* (Scer) Sec1p tail with homologues found in *Saccharomyces paradoxus* (Spar), *Saccharomyces bayanus* (Sbay), *Saccharomyces castellii* (Scas), *Schizosaccharomyces pompe* (Spom), *N. crassa* (Ncras), and *Mus musculus* (Mmus). The asterisk (*) marks identical, colon (:) strongly similar, and period (.) similar amino acids. Gray shading highlights similarity with Scer Sec1p. Black shading highlights positively charged amino acids in the C terminus of *S. pompe* and *N. crassa* Sec1p. (B) Alignment of the predicted secondary structures of the Sec1p tail. The secondary structure prediction was performed with the Psipred program (*Materials and Methods*). Bars represent predicted α-helixes. (C) Deletion of the Sec1p tail results in a temperature-sensitive growth phenotype in *sec1(1–657) MSO1-HA* cells. The growth of a serial 10-fold dilution series was scored at the indicated temperatures. (D) The spore formation is reduced in diploid *sec1(1–657)* cells. The quantification of tetrad formation in a minimum of 100 cells of *SEC1* wt (H2728) or *sec1(1–657)* (H3662) strains after synchronized spore formation. The average of results from three independent experiments is shown. (E) Blg2p accumulates in *sec1(1–657)* cells. Quantification of internally accumulated Bgl2p and a representative Western blot of *SEC1* wt (H2657) and *sec1(1–657)* (H3659) cells grown at 30°C or 37°C. Error bars represent the SD from three independent experiments.

time, even at the permissive temperature, deletion of the Sec1p tail caused loss of SNARE complex coprecipitation. Similar results were obtained when immunoprecipitations were performed with Sec1p-HA or Sec1p(1–657)-HA tagged at the genomic *SEC1* locus (unpublished data). These results suggest a positive role for the C-terminal tail in Sec1p-SNARE component interactions.

Reduced Sec1p binding with the membrane-anchored SNARE components would be expected to lead to increased levels of soluble Sec1p in the cytosol. To test this hypothesis, wt and *sec1(1–657)* cells were subjected to membrane fractionation. Compared to the wt Sec1p, there was 44% more Sec1p(1–657) in the cytosolic fraction (Figure 2B). When the distribution of Mso1p-HA was quantified in the same fractions, a 42% increase in Mso1p-HA levels was observed in the cytosolic fraction in *sec1(1–657)* mutant cells. At the same time, the transmembrane proteins Sso1/2p were detected only in the membrane pellet. The membrane fractionation results are in line with the observation that the coimmunoprecipitation efficiency of Mso1p-Sec1p(1–657) was not significantly affected by deletion of the tail (Figure 2A). These results suggest that Mso1p and Sec1p form a stable complex in the absence of the conserved C-terminal tail. When the strength of the Mso1p-Sec1p interaction was analyzed in vitro using the surface plasmon resonance technique with purified His_6-Mso1p and Sec1p, a relatively low K_d value of 3.4 nM indicating a strong binding was obtained (Supplemental Figure S3). This result is well in line with other findings suggesting that Mso1p and Sec1p form stable complexes (Castillo-Flores *et al.*, 2005; Knop *et al.*, 2005; Weber *et al.*, 2010).

Previously, using the bimolecular fluorescence complementation (BiFC) technique, Mso1p and Sec1p were shown to interact at sites of polarized growth and secretion (Weber *et al.*, 2010). Plasmids for expression of Mso1p fused with the C-terminal fragment of YFP (YFP(C)-Mso1p), and Sec1p or Sec1p(1–657) fused with the N-terminal fragment of Venus (Sec1p-Venus(N)) were transformed to wt yeast cells followed by analysis of the YFP signal. In haploid, vegetatively grown cells at 30°C, the signal for the Mso1p-Sec1p interaction site localized to the bud in 96% of the cells (Figure 2C). At the same time, 4% of the cells displayed a clearly detectable cytosolic signal over the background fluorescence. In Sec1p(1–657)-Venus(N)–expressing cells, in only 8% of the cells was an interaction with Mso1p detected in the bud by BiFC, whereas in 92% of the cells a cytosolic signal was observed. To obtain an index for the Mso1p-Sec1p interaction localization pattern, the signal intensity was measured for the Mso1p-Sec1p and Mso1p-Sec1p(1–657) interaction at the plasma membrane versus in the

cytosol. This measurement revealed that the Mso1p-Sec1p(1–657) complexes displayed a 1.6-fold enrichment in the cytosol. Collectively, these results point out a role for the Sec1p tail in SNARE complex binding.

The Sec1p tail interacts preferentially with ternary SNARE complexes

Previous results indicate that *S. cerevisiae* Sec1p binds preferentially assembled ternary SNARE complexes (Carr *et al.*, 1999; Scott *et al.*, 2004). Our results show that deletion of the C-terminal tail affected the coimmunoprecipitation of Sec1p and Mso1p with SNARE components (Figure 2A). To test whether the Sec1p tail can directly interact with SNARE components, binding of the Sec1p tail with the exocytic SNARE components was tested in vitro. To this end, pull-downs were performed by using purified maltose binding protein (MBP)-Sec1p(658–724) fusion protein bound to amylose resin that was incubated together with purified SNARE components alone or preassembled to binary (Sso1p-Sec9p) and tertiary (Sso1p-Sec9p-Snc2p) SNARE complexes. Binding between the Sec1p tail with both the binary and tertiary SNARE complexes was observed (Figure 3A, top panel, Coomassie-stained gel). Because of the partial masking of the bound Sso1p in the Coomassie-stained gel, the presence of Sso1p in the pulled-down samples was verified by Western blotting with anti-Sso1p specific antibodies (Figure 3A, bottom panel, Western blot with anti-Sso1p antibody). At the same time, no binding of the Sec1p tail with Sso1p (or Sso2p [unpublished data]) alone was evident. Quantification of the bound binary and tertiary complexes (10 μM) revealed that binding of the Sec1p tail to the tertiary complex was 72 ± 22% more efficient compared to binding to the binary complexes. The binding of the Sec1p tail to the binary and tertiary SNARE complexes was concentration dependent. A 3.3-fold increase in the amount of the binary and tertiary complexes (3 μM versus 10 μM) in the pull-down assay resulted in an increase of 83 ± 19% of pulled down binary and 33 ± 9% of pulled down tertiary complexes, respectively.

To genetically test the link between the Sec1p tail and SNARE complex components, *sec1(1–657) MSO1-HA* cells were transformed with the empty vector or plasmids overexpressing *SEC1*, *MSO1*, *SEC9*, *SSO1*, *SSO2*. Overexpression of the full-length *SEC1* or *MSO1* restored the ability of *sec1(1–657)* cells to grow even at 38°C (Figure 3B). At the same time, overexpression of the Q-SNAREs (*SEC9*, *SSO1*, and *SSO2*) was capable of restoring the growth at 37°C. At 38°C, *SSO2* was repeatedly a somewhat more efficient multicopy suppressor than *SSO1* (Figure 3B).

To assess the binding of the Sec1p tail with SNARE components in vivo, we made use of the BiFC technique. The wt yeast cells were transformed with plasmids expressing YFP(N)-Sso1p or YFP(N)-Sso2p together with Sec1p-YFP(C), Sec1p(1–657)-YFP(C), or Sec1p(658–724)-YFP(C) (Figure 3C). The signal indicating an interaction or close proximity between full-length Sec1p and Sso1p or Sso2p localized along the plasma membrane. No significant differences in the signal intensities were observed for Sec1p-Sso1p, Sec1p-Sso2p, or Sec1p(1–657)-Sso2p interaction. Compared to the Sec1p-Sso1p signal, however, a 78% reduction in the Sec1p(1–657)-Sso1p signal was observed (Figure 3C). Mso1p localizes together with Sec1p in the same complexes with Sso1p and Sso2p, and this interaction can be detected with BiFC (Weber *et al.*, 2010). When the Mso1p-Sso1/2p BiFC signal was examined in *sec1(1–657)* cells, similarly to Sec1p(1–657)-Sso1p a clear reduction in the Mso1p-Sso1p signal was observed (Supplemental Figure S4). At the same time, the Sso2p-Mso1p signal persisted. Coexpression of just the Sec1p tail [Sec1p(658–724)-YFP(C)] with YFP(N)-Sso1p or Sso2p resulted in a clear BiFC signal at the plasma membrane. The BiFC signal was 22% stronger, however, for Sec1p(658–724)-Sso1p complexes than for Sec1p(658–724)-Sso2p (Figure 3C). To test Sec1p tail-Sso1p binding in a different way, yeast two-hybrid assays were performed. In these assays, weak binding was observed between the Sec1p tail (658–724) and Sso1p or Sso2p lacking their transmembrane domain (Figure 3D). In line with the BiFC results and genetic interactions, the binding was slightly stronger for the Sec1p tail with Sso1p than with Sso2p.

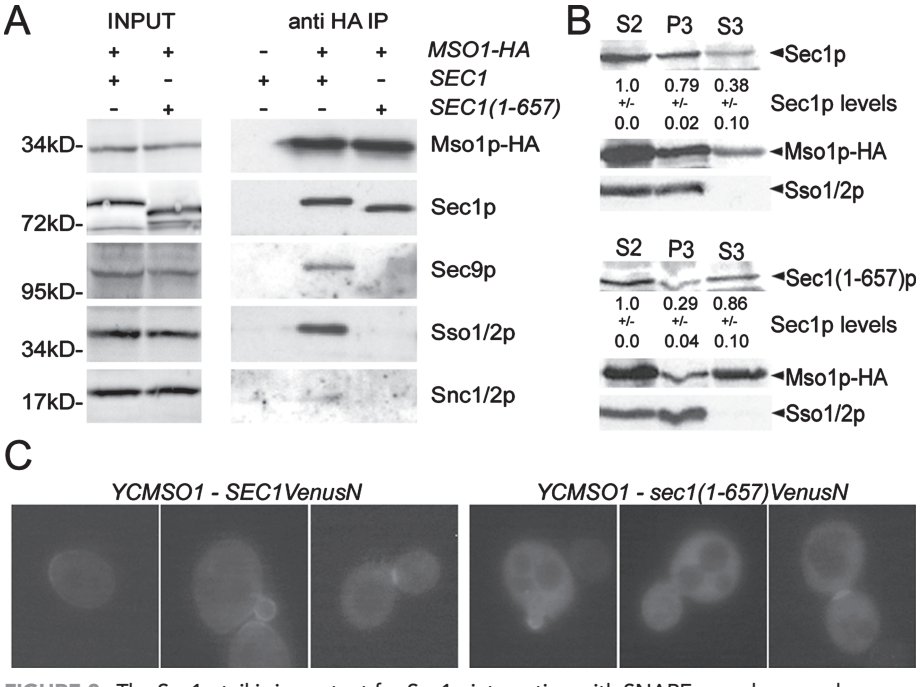

FIGURE 2: The Sec1p tail is important for Sec1p interaction with SNARE complexes and membrane association in vivo. (A) The Sec1p C-terminal tail is needed for Sec1p coimmunoprecipitation with SNARE components. *MSO1-HA* cells expressing wt *SEC1* or mutant *sec1(1–657)* cells were grown until $OD_{600} = 1$, lysed, and subjected to anti-HA immunoprecipitations. Immunoprecipitates were analyzed by Western blotting with anti-HA, -Sec1p, -Sec9p, -Sso1p/2p, and -Snc1p/2p antibodies. (B) Sec1p(1–657) has reduced membrane association. Membranes were fractionated by differential centrifugation and analyzed by Western blotting and detection with anti-HA, -Sec1p, and -Sso1p/2p antibodies. S2, the supernatant after centrifugation at 10,000 × *g*, P3, the pellet after centrifugation at 100,000 × *g* and S3, the supernatant after centrifugation at 100,000 × *g*. The Sec1p (wt and 1–657) signal from three independent experiments was quantified and normalized to the amount of Sec1p in the S2 fraction. (C) Localization of the Mso1p interaction site with Sec1p and Sec1p(1–657) in vivo. Haploid, vegetatively grown cells (H304) expressing YFP(C)-Mso1p (*CEN*, *MET25* promoter, B3044) and Sec1p-Venus(N) (*CEN*, *ADH1* promoter, B2930) or Sec1p(1–657)-Venus(N) (*CEN*, *ADH1* promoter, B3279) were investigated by fluorescence microscopy. The distribution of the BiFC signal was analyzed in a minimum of 70 cells per interaction mode.

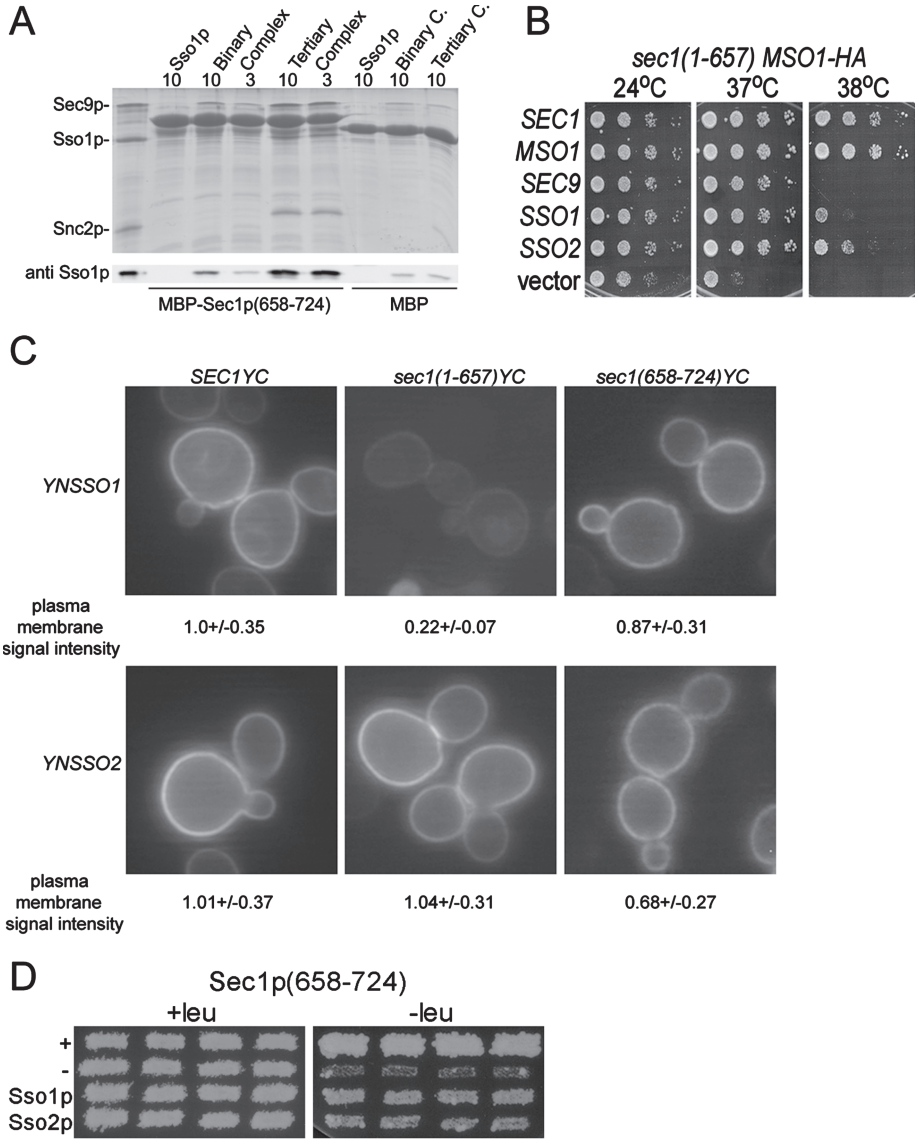

FIGURE 3: The analysis of Sec1p tail interactions with SNARE components and complexes. (A) MBP-Sec1p(658–724) binds to the binary and tertiary SNARE complex in vitro. MPB-Sec1p(658–724) bound to amylose resin was mixed with the indicated amounts of Sso1p, Sso1p-Sec9p binary, and Sso1p-Sec9p-Snc2p tertiary complexes and incubated at room temperature for 1 h. Bound proteins were separated by SDS–PAGE and stained with Coomassie Brilliant Blue. MBP served as a negative control. A representative gel of three independent experiments is shown. In the bottom panel, the presence of Sso1p in the pull-down was verified by Western blotting with anti-Sso1p antibodies. (B) The temperature-sensitive growth defect of the *sec1(1–657) MSO1-HA* strain is rescued differentially by the overexpression of *SEC1* and *MSO1, SSO1*, or *SSO2*. The growth of a serial 10-fold dilutions of cells grown at the indicated temperatures is shown. (C) Localization and intensity of the interaction of different versions of Sec1p with Sso1/2p in vivo. Haploid, vegetatively grown cells (H304) expressing YFP(N)-Sso1p (2μ, *ADH1* promoter, B3307), YFP(N)-Sso2p (2 μ, *ADH1* promoter, B3309) together with different mutant versions of Sec1p-YFP(C) (2μ, *ADH1* promoter) (wt (B3308), Sec1p(1–657) (B3311), Sec1p(658–724) (B3406)) were investigated by fluorescence microscopy. (D) Interactions between Sec1p(658–724) and Sso1p or Sso2p in the yeast two-hybrid assay. The growth of four independent colonies per interaction mode is shown on medium with or without leucine. The bicoid (B1228) was used as a negative control and Gal4 (B1229) as a positive control.

The Sec1p tail promotes Sec1p-SNARE association and in vitro assembly of SNARE complexes

To shed light on the Sec1p tail in vivo function we created a *SEC1(658–724)* overexpression construct and analyzed the contribution of the Sec1p tail on Sec1p-SNARE complex interaction in wt and *sec1(1–657)* mutant cells. Under the conditions tested, overexpression of *SEC1(658–724)* was clearly not harmful for cell growth (Figure 4A, top panel). Instead, compared to the vector control, overexpression of *SEC1(658–724)* was mildly beneficial for growth of the *sec1(1–657)* mutant strain at all temperatures (Figure 4A, bottom panel).

Deletion of the Sec1p tail reduced coimmunoprecipitation of Mso1p and Sec1p with SNARE components (Figure 2A). To test the effect of Sec1p(658–724) overexpression on the Sec1p coimmunoprecipitation with Mso1p and SNARE components, anti-HA immunoprecipitations were performed with lysates in which Mso1p was HA-tagged and the Sec1p tail (658–724) was overexpressed. Overexpression of Sec1p(658–724) could not restore SNARE complex coimmunoprecipitation in the *sec1(1–657)* mutant strain (unpublished data). In the wt *SEC1* strain, however, Sec1p tail overexpression caused increased coprecipitation of Sec9p (87% more) and Sso1/2p (63% more) with Mso1p-HA (Figure 4, B and C). In the same immunoprecipitations, overexpression of the Sec1p tail had only a moderate effect on Sec1p coimmunoprecipitation with Mso1p (12% more). Similar results were obtained in immunoprecipitations of HA-tagged Sec1p (unpublished data).

To directly analyze SNARE complex levels in cells lacking the Sec1p C-terminal tail or overexpressing it, immunoprecipitation experiments were carried out with cell lysates in which an N-terminal myc-tagged Snc2p was expressed from a plasmid. Compared to Sec1p tail mutant cells grown at 30°C, deletion of the Sec1p tail caused a 35% reduction in coimmunoprecipitation of Sso1/2p with myc-Snc2p at 37°C (Supplemental Figure S5A). At the same time, in wt cells grown at 37°C, the coimmunoprecipitation of Sso1/2p with myc-Snc2p was reduced only by 10% when compared to wt cells grown at 30°C. These results suggest that, although the Sec1p C-tail has a positive role for Sec1p-SNARE component interactions, its deletion only moderately affects the amount of assembled SNARE complexes. The overexpression of the Sec1p tail in a wt strain slightly enhanced Sso1/2p coimmunoprecipitation with myc-Snc2p (12% more; Supplemental Figure S5B). This finding suggests that the Sec1p tail does not compete with full-length Sec1p, but instead when overexpressed it improves the assembly and coimmunoprecipitation of Mso1p-Sec1p-SNARE complexes.

The putative positive role for the Sec1p tail in SNARE complex assembly was tested with purified components in vitro. To this end, native gel mobility assays were performed with Sso1p, Snc2p,

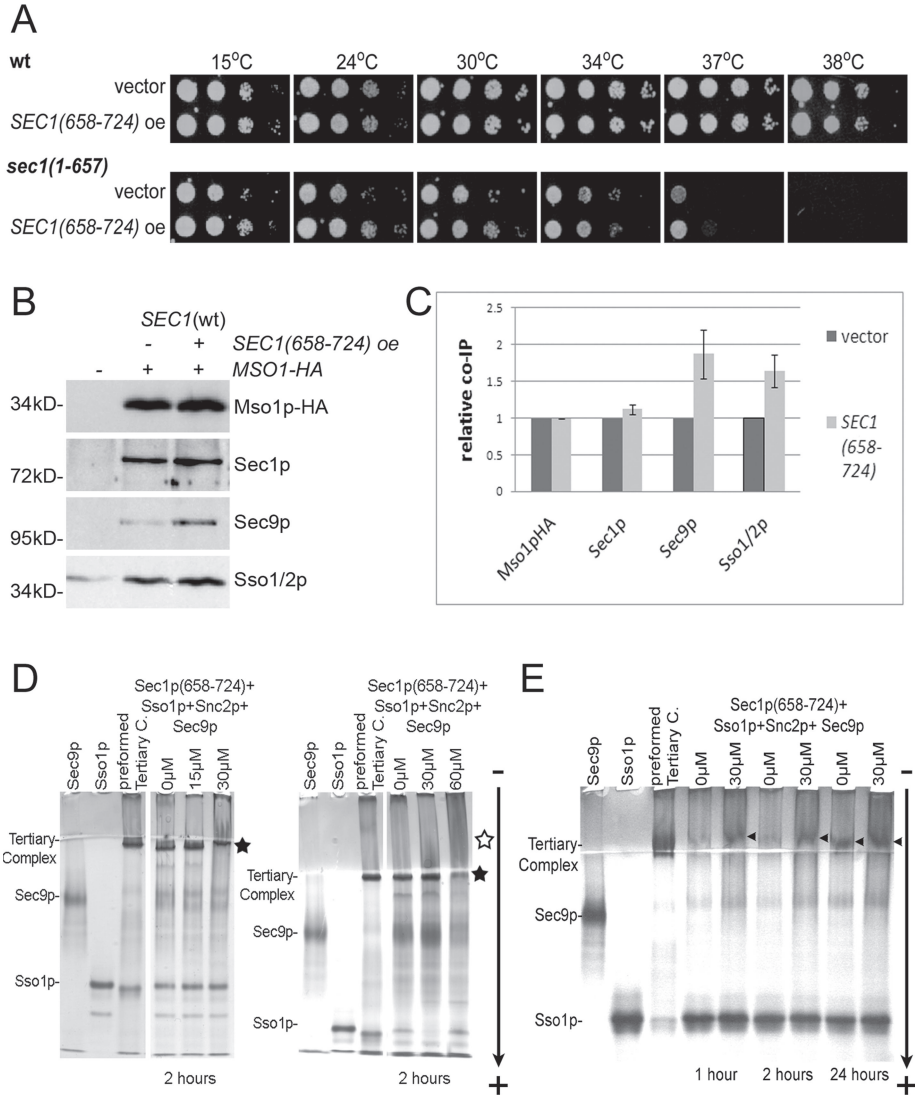

FIGURE 4: The Sec1p-tail promotes Sec1p-SNARE complex association. (A) The effect of *SEC1(658–724)* (B3424) overexpression for growth in *SEC1* wt (H2657) and *sec1(1–657)* mutant (H3659) strains. The growth of serial 10-fold dilutions of cells grown at the indicated temperatures is shown. (B) Sec1p tail overexpression enhances coimmunoprecipitation of SNARE complexes with Mso1p-HA. *MSO1-HA* cells (H2657) overexpressing *SEC1(658–724)* (B3424) were grown until OD_{600} = 1, lysed, and subjected to anti-HA immunoprecipitations. Immunoprecipitates were analyzed by Western blotting with anti-HA, -Sec1p, -Sec9p, and -Sso1p/2p antibodies. (C) Quantification of three independent experiments of immunoprecipitations shown in (B). (D) Sec1p(658–724) promotes SNARE complex formation in vitro. Sso1p, Snc2p, Sec9p (30 µM each), and indicated amounts of His_6-Sec1p(658–724) were mixed and incubated at room temperature for 2 h. The complex formation was analyzed by native gel. The 8% native gels were run from the – to the + pole. The black star indicates the position of ternary complexes, and the open star other complexes. (E) Kinetics of the Sec1p(658–724) effect on SNARE complex formation in vitro. Gel mobility assays were performed essentially as in (D) with the exception that proteins were incubated at 4°C for 1, 2, or 24 h. The arrowheads indicate the position of ternary complexes.

Sec9p, and increasing amounts of purified His_6-Sec1p(658–724). After a 2-h incubation at room temperature and subsequent analysis in a native gel, a 70% increase in tertiary SNARE complex formation could be observed when a subequimolar concentration of the Sec1p tail [15 µM Sec1p(658–724):30 µM SNARE components] was used (Figure 4D, left panel). Equimolar concentrations (30 µM) resulted in slower mobility of the ternary SNARE complexes (Figure 4D, left panel, star). This increase of mobility could be due to the association of the positively charged Sec1p tail with the SNARE complexes. The identity of the ternary complexes (presence of Sso1p, Sec9p, and Snc2p) was verified by matrix-assisted laser desorption ionization mass spectrometry (MALDI MS) (unpublished data). An increase of the Sec1p tail to 60 µM versus 30 µM SNARE components resulted in the formation of complexes of reduced mobility (Figure 4D, right panel, open star). At the same time, the amount of ternary complexes was reduced (Figure 4D, right panel, black star). At room temperature, a significant amount of SNARE complex assembly took place in 2 h. To gain better understanding of the effect of the Sec1p tail in SNARE complex assembly, experiments in the presence or absence of the Sec1p tail were performed at 4°C with equimolar concentrations of the components. The results show that addition of the Sec1p tail resulted in SNARE complex formation at the 1-h time point (Figure 4E, black arrowhead). At the same time point, in the sample without the Sec1p tail, clearly fewer SNARE complexes were observed (Figure 4E). Irrespective of the presence or absence of the Sec1p tail, after 24 h at room temperature or at 4°C the samples contained SNARE complexes (Figure 4, D and E). At both temperatures, however, more efficient complex formation tvook place in the presence of the Sec1p tail. Collectively, the results suggest that Sec1p tail binding to SNARE complexes results in improved SNARE complex coimmunoprecipitation in vivo and enhanced SNARE complex formation in vitro.

Mso1p can facilitate the polarized localization of Sec1p lacking its C-terminal tail

In contrast to the polarized localization in wt cells, in *sso2–1 Δsso1* SNARE mutant cells the Mso1p-Sec1p BiFC signal becomes distributed throughout the plasma membrane (Weber *et al.*, 2010). We made use of this feature to test whether the Sec1p tail is important for the plasma membrane association of Mso1p-Sec1p complexes in their widely distributed plasma membrane location in *sso2–1 Δsso1* cells, when presumably the amounts of other components contributing to SNARE complex assembly are not present in as high amounts as compared to the wt cell situation in which Mso1p-Sec1p complexes have a focal localization in the tip of the wt cell bud. To this end, *sso2–1 Δsso1* cells were transformed with plasmids expressing YFP(C)-Mso1p and Sec1p-Venus(N) or Sec1p(1–657)-Venus(N), and the BiFC signal localization was examined. As reported previously, the BiFC signal for the Mso1p-Sec1p interaction localized throughout the plasma membrane in 82% of the cells. In 18% of the cells, a more prominent signal was observed in the growing bud (Figure 5, A and B). To our surprise, when the interaction site for Mso1p-Sec1p(1–657) was

analyzed in *sso2–1 Δsso1* cells, 84% of the cells displayed a prominent polarized localization of the BiFC signal in the bud (Figure 5, A and B). At the same time, none of the cells displayed a clearly detectable BiFC signal that localized throughout the plasma membranes of both the mother and daughter cells. This finding raises the possibility that, in *sso2–1 Δsso1* cells, the compromised SNARE complexes and the reduced SNARE binding by the deletion of the Sec1p C terminus reveals an additional targeting mechanism for Mso1p-Sec1p(1–657) complexes.

We have shown that the amino acids 38–59 in Mso1p comprise the minimal region required for Sec1p binding (Knop *et al.*, 2005). To identify the part of Mso1p required for the polarized localization of the Mso1p-Sec1p(1–657) interaction site BiFC assays were performed in *sso2–1 Δsso1* cells. For these assays we made use of the mutant versions of Mso1p that contain the Sec1p binding site, but where the C terminus of Mso1p was deleted. In *sso2–1 Δsso1* cells that express *YFP(C)-MSO1(1–135)* or *YFP(C)-MSO1(1–188)* and the full-length *SEC1-Venus(N)* from plasmids, a similar localization for the BiFC signal was observed as in cells expressing the full-length Mso1p and Sec1p (Figure 5, A and B). For Mso1p(1–135)-Sec1p(1–657) and Mso1p(1–188)-Sec1p(1–657), however, a shift in the localization of the BiFC signal to the cytosol was observed (Figure 5, A and B). Only 3% of the cells showed an interaction signal at the growing bud, whereas 97% displayed a cytosolic signal. This result shows that the last 22 amino acids of Mso1p are important for the polarized membrane targeting of the Mso1p-Sec1p(1–657) complexes in *sso2–1Δ sso1* cells.

To analyze the function of the Mso1p C terminus in vivo, a strain was generated that expressed *mso1(1–188)* as the only copy of *MSO1* (from its own promoter). The haploid and homozygous diploid *mso1(1–188)* mutant cells were viable, and, for haploid cells, no phenotypes were observed in different growth conditions tested (unpublished data). When *mso1(1–188)/mso1(1–188)* diploid cells were induced to sporulate, a delay in spore formation was observed (Figure 5C). After 24 h, however, both the wt and *mso1(1–188)* mutant strain reached similar levels of tetrad formation. This result suggests that deletion of the Mso1p C terminus results in a slowed down formation of the prospore membrane.

Mso1p binds Sec4p in vitro and colocalizes with Sec4p(Q79L) on intracellular membranes

Previously it was observed that, even at the permissive temperature, deletion of *MSO1* was lethal in combination with the *sec4–8* temperature-sensitive mutation (Knop *et al.*, 2005). Sec4p is a small Rab-GTPase implicated in the polarized targeting of secretory vesicles (Goud *et al.*, 1988; Guo *et al.*, 1999). The strong genetic link between *MSO1* and the *sec4–8* mutation was not dependent on Mso1p binding to Sec1p, but instead the results pointed to a role for Mso1p C terminus in this genetic interaction (Knop *et al.*, 2005). In addition to the genetic link with *sec4–8*, *MSO1* deletion formed a lethal combination with a temperature-sensitive mutation in the Sec4p GEF Sec2p (Knop *et al.*, 2005). These findings raise the possibility that Mso1p cooperation with an activated Sec4p is needed prior to exocytosis. This finding prompted us to investigate whether an interaction between Mso1p and Sec4p could be observed and whether this interaction could contribute to the polarized targeting of Mso1p.

To test if Mso1p can interact with Sec4p in vitro pull-down assays were performed with purified components. For these assays MBP-Sec4p-CC was bound to amylose resin and incubated with γGTP and the N-terminally tagged, purified Mso1p. As negative controls, binding reactions with the tags alone were carried out. Although the tags alone did not interact with Sec4p, binding between Mso1p and Sec4p-CC was observed (Figure 6A, top panel, Western blot). These results suggest that Mso1p can directly interact with a GTP loaded Sec4p in vitro.

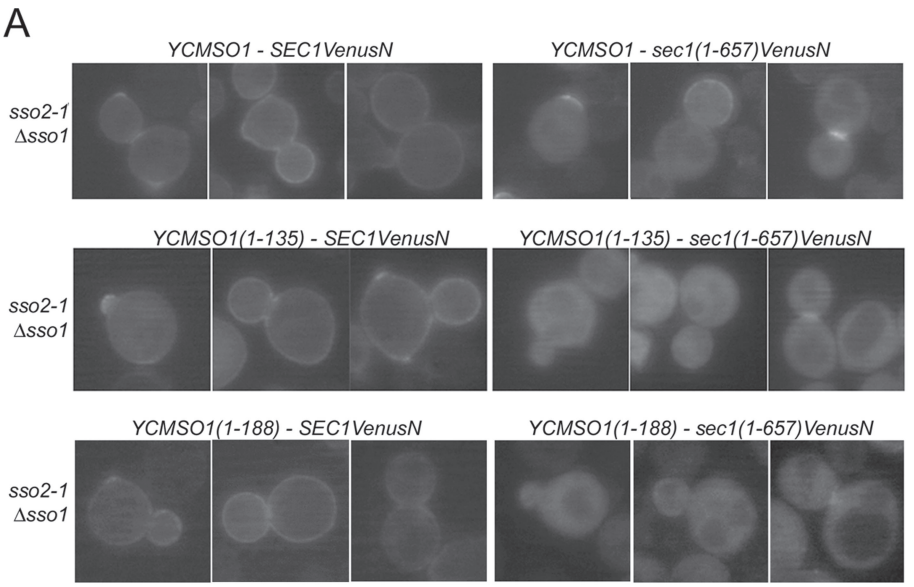

B

Distribution of the BiFC signal

examined BiFC constructs	growing bud	membrane	cytosol
YCMSO1(1-210)-SEC1(1-724)VN	0.18	0.82	0
YCMSO1(1-210)-sec1(1-657)VN	0.84	0	0.16
YCMSO1(1-135)-SEC1(1-724)VN	0.10	0.90	0
YCMSO1(1-135)-sec1(1-657)VN	0.03	0	0.97
YCMSO1(1-188)-SEC1(1-724)VN	0.09	0.91	0
YCMSO1(1-188)-sec1(1-657)VN	0.03	0	0.97

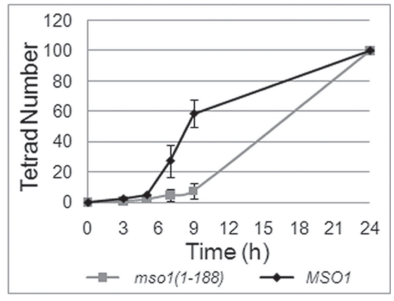

FIGURE 5: The Mso1p C terminus can mediate polarized localization of Sec1p(1–657)-Mso1p complexes in *sso2–1 Δsso1* mutant cells. (A) BiFC analysis of haploid *sso2–1 Δsso1* cells (H1152) expressing YFP(C)-Mso1p (*CEN*, *MET25* promoter, B3044), YFP(C)-Mso1p(1–135) (*CEN*, *MET25* promoter, B3354), or YFP(C)-Mso1p(1–188) (*CEN*, *MET25* promoter, B3556) together with either Sec1p-Venus(N) (*CEN*, *ADH1* promoter, B2930) or Sec1p(1–657)-Venus(N) (*CEN*, *ADH1* promoter, B3279). (B) The distribution of the BiFC signal in (A) was analyzed in a minimum of 50 cells per interaction mode. (C) The Mso1p C terminus is necessary for normal sporulation. The number of tetrads formed in *mso1(1–188)* cells (H3490) is displayed as a function of time. A minimum of 100 cells per strain were examined for tetrad formation at the indicated time points after synchronized spore formation induction. Results from four independent experiments are shown.

To analyze the possible interactions of Mso1p with Sec4p in vivo, we made use of the BiFC assay. We used the wt, guanosine diphosphate (GDP) locked (S34N), GTP locked (Q79L), and no nucleotide binding (N133I) versions of Sec4p to address the interaction of Mso1p with Sec4p. Haploid wt yeast cells were transformed with plasmids expressing YFP(C)-Mso1p and different versions of YFP(N)-Sec4p (wt, S34N, Q79L, and N133I). A BiFC signal was observed at the septum and in the growing bud for Mso1p-Sec4p(wt) and Sec4p(Q79L) (Figure 6B). The Sec4p(S34N) mutant showed only a weak BiFC signal with Mso1p in the septum. No BiFC signal was observed for the Mso1p-Sec4p(N133I) pair. This finding suggests that Mso1p is found in close proximity to the GTP-bound Sec4p in vivo. A highly similar interaction profile was seen for the different Sec4p mutants with Sec9p, a known effector of Sec4p (Brennwald *et al.*, 1994) (Supplemental Figure S6A). Together with the genetic and in vitro results, this finding suggests that Mso1p may act in close cooperation with Sec4p in vivo.

The Mso1p-Sec4(Q79L) BiFC signal was frequently detected in structures that appeared to localize inside the bud, away from the plasma membrane (Figure 6B, arrow). To gain improved resolution of the Mso1p-Sec4p (wt and Q79L) BiFC signal inside the bud, larger diploid yeast cells were transformed with Mso1p-Venus(C) and YFP(N)-Sec4p(Q79L) plasmids. In these cells, the Mso1p-Sec4p(Q79L) BiFC signal was observed in dotty structures in emerging and small growing buds (Figure 6C, 1 and 2, arrows). In bigger buds, the signal was often detected as separate small dots close to and along the plasma membrane (Figure 6C, 3 and 4). At the same time, an increase of the BiFC signal at the plasma membrane was observed. In cells undergoing cytokinesis, no dotty structures at the plasma membrane were observed, but instead the Mso1p-Sec4p(Q79L) BiFC signal decorated the septum of dividing cells (Figure 6C, 5). In cells expressing the Mso1p-Sec4p(N133I) pair, a negligible BiFC signal was detected (Figure 6C, 6).

When the diploid cells were followed over time, regularly, elements positive for the Mso1p-Sec4p(Q79L) BiFC signal with a dynamic behavior were observed close to the plasma membrane (Figure 6D, arrows). Occasionally, these elements were seen to merge with the plasma membrane and ultimately disappear (Figure 6D, arrowheads). When the requirement of the N and C terminus of Mso1p for the Mso1p-Sec4p(Q79L) BiFC signal was tested, it was observed that the C-terminal half of Mso1p [Mso1p(136–210)] displayed a BiFC signal with Sec4p(Q79L) only in the intracellular structures and the septum (Supplemental Figure S6B). At the same time, the Mso1p(1–135)-Sec4p(Q79L) signal localized similarly as did the full-length Mso1p-Sec4p(Q79L) signal. Taken together, these results suggest that Mso1p can reside in close proximity to Sec4p on the intracellular membrane structures close to the plasma membrane.

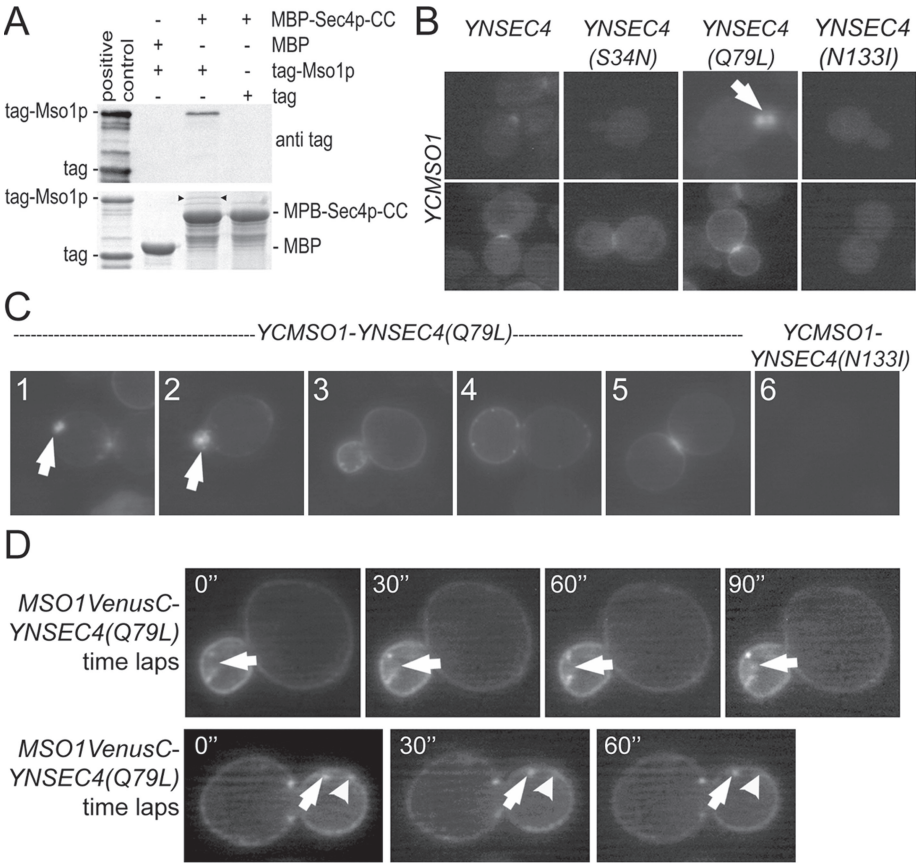

FIGURE 6: Mso1p binds Sec4p in vitro and colocalizes with GTP-bound Sec4p on membrane structures in the bud. (A) Mso1p binds to Sec4p-CC in vitro. MPB-Sec4p-CC (4 μM) bound on amylose resin was mixed with 10 μM γGTP, 0.5% NP-40, and 8 μM N-terminally tagged Mso1p or the tag alone and incubated at room temperature for 2 h. Bound proteins were separated by SDS–PAGE. The gels were either subjected to Western blotting with antibodies against tagged Mso1p (top panel) or stained with Coomassie (bottom panel). As a positive control, Mso1p and the tag alone were loaded in the gel in the same lane (the first lane from left). A representative gel of several repeats is shown. Arrowheads point to the position of Mso1p bound to Sec4p in the Coomassie Blue–stained gel. (B) Mso1p localizes in close proximity with wt or GTP-bound Sec4p on intracellular membranes. Vegetatively grown haploid cells (H304) expressing YFP(C)-Mso1p (*CEN*, *MET25* promoter, B3044) and YFP(N)Sec4p (2 μ, *ADH1* promoter) [wt (B3316), S34N (B3318), Q79L (B3317), N133I (B3319)] were examined for BiFC signal. Arrows point to BiFC signal inside the bud. (C) Live cell imaging of diploid (H2530) cells expressing Mso1p-Venus(C) (*CEN*, *ADH1* promoter, B2918) and YFP(N)Sec4p (2 μ, *ADH1* promoter) (Q79L (B3317), N133I (B3319)). Arrows point to BiFC signal inside the bud. (D) Time series of the intracellular BiFC signal in the same strain as used in (C). Arrow points to intracellular membrane structure positive for Mso1p-Sec4p proximity. The arrowhead indicates a plasma membrane site of BiFC element disappearance.

Mso1p-Sec4p colocalization is dependent on Sec2p and does not require a functional exocytic SNARE complex

To position the Mso1p-Sec4p interaction in the cascade leading to vesicle fusion at the plasma membrane, the Mso1p-Sec4p BiFC signal was analyzed in different temperature-sensitive mutants. In wt cells, the Mso1p-Sec4p BiFC signal localized similarly to the bud and the septum area both at the permissive temperature 24°C and the restrictive temperature 37°C (Figure 7A). This polarized localization of the Mso1p-Sec4p BiFC signal was also observed in *sso2–1 Δsso1* cells grown at the restrictive temperature 30°C (Figure 7B). This temperature completely inhibits growth through inactivation

of the exocytic SNARE complexes (Jantti *et al.*, 2002). The result suggests that in a situation where SNARE complexes are functionally compromised, the Mso1p-Sec4p proximity is still maintained. Sec2p is a GEF for Sec4p required for GTP loading in Sec4p. In *sec2–41* cells, a 34% reduction of the Mso1p-Sec4p BiFC signal was observed in the bud at the permissive temperature (25% versus 38%, Figure 7C). This effect became more pronounced at the restrictive temperature (74% less, 10% versus 38%). This result suggests that fully functional GTP loading for Sec4p is important for the Mso1p-Sec4p association. This result, together with the BiFC results with Sec4p(Q79L), suggests that in vivo Mso1p cooperates preferentially with the GTP-bound Sec4p.

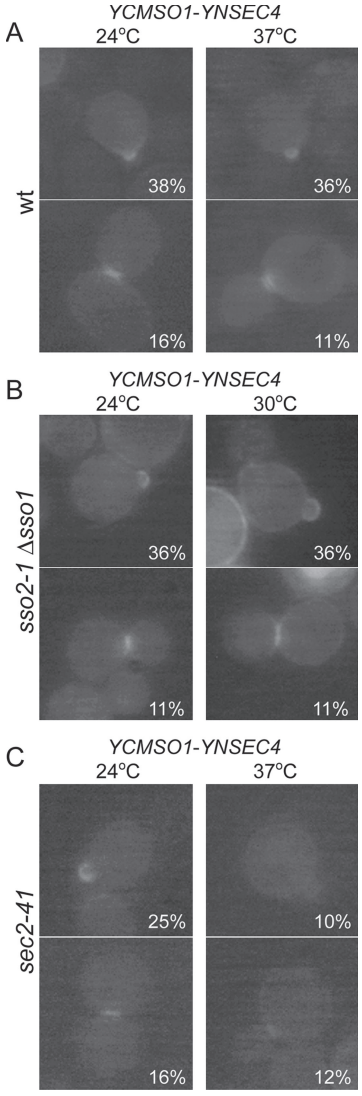

FIGURE 7: Mso1p-Sec4p colocalization is depended on Sec2p and independent of a functional SNARE complex. (A) wt, (B) *sso2–1 Δsso1*, and (C) *sec2–41* cells coexpressing YFP(C)-Mso1p (*CEN, MET25* promoter, B3044) and YFP(N)-Sec4p (*2μ, ADH1* promoter, B3316) were grown to OD_{600} = 0.8–1 at 24°C, and the cultures were split and either left at 24°C or shifted to the indicated restrictive temperature for 1 h prior to investigation. For each condition, the signal localization was quantified in at least 50 cells. The numbers in the figures indicate the percentage of cells showing Mso1p-Sec4p localization in the bud (top panels) or septum (bottom panels), respectively.

DISCUSSION

According to the current model, there is an initial step of recognition and docking of transport vesicles at the target membrane by a tethering complex (Jahn and Scheller, 2006). In the case of plasma membrane, this function is carried out by the exocyst complex (Munson and Novick, 2006; He and Guo, 2009). It has been shown that Sec2p and Sec4p can interact with the exocyst subunit Sec15p and thus could be involved in the formation of a docking complex at the plasma membrane (Walch-Solimena *et al.*, 1997; Guo *et al.*, 1999; Mizuno-Yamasaki *et al.*, 2010). It is not known how a transport vesicle is transferred from the docking complex to the assembly phase of the SNARE complexes and membrane fusion. It is conceivable, however, that in this process molecular mechanisms exist that ensure a directional assembly of the components. The results in this study characterize two molecular interaction modes that participate in this process.

The molecular mechanisms of membrane fusion are well conserved in evolution, and functionally essential proteins in the membrane fusion process are known. SM protein family members are central for SNARE complex regulation (Toonen and Verhage, 2003). A large body of work has revealed several modes of interaction between SM proteins and syntaxins (Carr *et al.*, 1999; Misura *et al.*, 2000; Bracher and Weissenhorn, 2002; Dulubova *et al.*, 2002; Peng and Gallwitz, 2002; Yamaguchi *et al.*, 2002; Gallwitz and Jahn, 2003; Scott *et al.*, 2004; Carpp *et al.*, 2006; Latham *et al.*, 2006; Togneri *et al.*, 2006; Hu *et al.*, 2007; Shen *et al.*, 2007; Toonen and Verhage, 2007; Deak *et al.*, 2009; Furgason *et al.*, 2009; Munson and Bryant, 2009; Carr and Rizo, 2010). A common feature in these different interaction modes is that SM proteins possessing an arch-shaped structure interact with syntaxins either within the arch cavity or through the binding of domain 1 with an N-terminal peptide of syntaxins (Munson and Bryant, 2009; Carr and Rizo, 2010). The current data suggest that the syntaxin N-terminal peptide interaction with SM proteins is a widely used mode of interaction between these molecules. The exocytic syntaxins Sso1p and Sso2p in *S. cerevisae* do not possess an N-terminal peptide. Instead, the Sec1p domain 1 interacts with Mso1p (Weber *et al.*, 2010). Mso1p can also bind to Sso1p and may therefore mimic the role of the N-peptide.

In contrast to its homologues in higher eukaryotes, the *S. cerevisiae* Sec1p possesses an extended C-terminal tail. This C-terminal peptide is well conserved in fungal Sec1p homologous. Our in vitro results show that this peptide can interact with binary Sec9p-Sso1p and ternary Snc2p-Sec9p-Sso1p complexes. Previous studies of Sec1p binding with Sso proteins or SNARE complexes have shown a similar binding preference for the full-length Sec1p (Scott *et al.*, 2004). Our results show that the C-terminal peptide also has a role in vivo. Deletion of the 67 last amino acids of Sec1p resulted in temperature-sensitive growth of haploid cells, intracellular accumulation of Bgl2p, and significantly defective sporulation. Sporulation is dependent on prospore membrane formation that requires homotypic membrane fusion of transport vesicles that are targeted to the spindle pole body (Neiman, 1998; Knop *et al.*, 2005; Neiman, 2005). Interestingly, no obvious secretion phenotype was observed for Hsp150. Bgl2p and Hsp150 have been suggested to use different types of vesicles for their transport to the plasma membrane, Bgl2p in light-density vesicles and Hsp150 in high-density vesicle with, for example, invertase (Harsay and Bretscher, 1995; Nunes Bastos, 2008). These results raise the interesting possibility that Sec1p tail is differentially important for the fusion of different types of transport vesicles.

Whereas Sec1p lacking its C terminus interacts with Mso1p like the wt Sec1p, a significantly reduced affinity to SNARE components

in coimmunoprecipitation experiments for the tail mutant was observed. In contrast to this finding, overexpression of the Sec1p tail enhanced Sec1p coimmunoprecipitation with the SNAREs (Figure 4, B and C). In BiFC assays, a clear difference was observed between the signal intensity for Sso1p or Sso2p with the Sec1p tail mutant (Figure 3C). This observation could reflect a contribution of the Sec1p tail, especially for interactions with Sso1p. This hypothesis is supported by the multicopy suppression and the yeast two-hybrid results (Figure 3, B and D). Previous results have shown that, in meiotic diploid cells, Sso1p, but not Sso2p, is needed for the fusion of prospore membrane vesicles (Jäntti *et al.*, 2002; Knop *et al.*, 2005). Clearly, additional experiments are needed to verify the differential interplay between Sso1p, Sso2p, and Sec1p in vegetatively grown haploid cells and to confirm whether Sso1p- or Sso2p-containing SNARE complexes can play differential roles in membrane fusion of different types of vesicles in exocytosis.

Based on the published SM protein structures, it appears feasible that the C-terminal peptide localizes in the cavity side of the Sec1p arch and would therefore be well positioned to contribute to SNARE binding. The C-terminal peptide does not possess any obvious sequence motifs. *S. cerevisiae* Sec1p, however, contains 16 lysine and arginine residues and has a net positive charge (pI 10.3) at the cytosolic pH. It is interesting to note that the surface of SNARE complexes is negatively charged (Strop *et al.*, 2008). It is therefore possible that the observed interaction of the Sec1p tail with SNARE complexes is at least partially mediated by ionic interactions. Of the *S. cerevisiae* SM proteins–Sly1p, and Vps45p, and Vps33p–Vps33p has an approximately 30-amino-acid-long C-terminal tail (Supplemental Figure S1). Although clearly shorter than the Sec1p tail, it is also positively charged (pI 11.2). It is noteworthy that, whereas the syntaxins interacting with Sly1p and Vps45p possess an N-terminal peptide, the binding partners for Vps33p and Sec1p lack them. These results raise the possibility that at least in *S. cerevisiae* the negatively charged C-terminal peptides can provide, in the absence of the syntaxin N-peptides, additional affinity for SM protein-syntaxin complexes. *S. pombe* and *N. crassa* have clearly negatively charged Sec1p C-terminal tails (Figure 1A). It is therefore likely that the functional role of the Sec1p tail is used widely in eukaryotic species. In mammalian cells, however, none of the SM proteins possess a C-terminal peptide. It could be that in mammalian cells other SM and syntaxin binding proteins (not present in fungal species) can positively contribute to SNARE complex formation.

Our results reveal a role for the nonconserved Sec1p C-terminal tail and suggest a model in which the Sec1p C-terminal peptide can positively affect the assembly of SNARE complexes. In the absence of the N-terminal peptide in Sso syntaxins, this added affinity, together with the Sec1p interaction with Mso1p, could offer a framework of molecular interactions that enable the dynamic and directional assembly of SNARE complexes.

A shift in the localization of the BiFC signal between Mso1p and Sec1p lacking its C-terminal tail, together with the previously observed synthetic lethality between *MSO1* and *sec4–8* mutations, prompted us to test whether Sec4p could be involved in the targeting of Mso1p to sites of polarized exocytosis. The results suggest that Mso1p may act as an effector for Sec4p. This idea is supported by results showing a direct interaction between Mso1p and Sec4p in vitro. Furthermore, such a link is supported by in vivo findings using the BiFC technique. The Sec4p-Mso1p BiFC signal was especially prominent for the presumably GTP locked form of Sec4p(Q79L). For the GDP-locked form Sec4p(S34N) and Mso1p only a weak signal was detected. Further support for the importance of the nucleotide binding state of Sec4p for the BiFC signal with Mso1p was evident when this signal was clearly reduced in *sec2–41* cells that are defective for the Sec4p GEF Sec2p (Walch-Solimena *et al.*, 1997). Our results indicate that the C-terminal part (amino acids 136–210) of Mso1p is important for the BiFC signal with Sec4p(Q79L) in intracellular elements (Supplemental Figure S6B). The role of the Mso1p C terminus for Sec4p cooperation is supported both by in vivo binding experiments and genetic results that show that Mso1p mutants that are defective for the Sec1p binding domain located at the N terminus of Mso1p can still rescue the synthetic lethal phenotype in *sec4–8 Δmso1* cells (Knop *et al.*, 2005). When the BiFC signal for the known Sec4p effector Sec9p was analyzed, it was evident that this protein pair displays a signal distribution and nucleotide binding dependence similar to those of Mso1p and Sec4p (Supplemental Figure S6A). This finding suggests that Sec4p effectors can meet Sec4p in intracellular membrane structures prior to arrival at the plasma membrane.

Our results suggest the existence of a network of protein–protein interactions that control the docking of transport vesicles and the formation of SNARE complexes (Figure 8). The fact that Sec1p overexpression can bypass the functions of the exocyst docking complex subunits Sec3p, Sec5p, and Exo70p, together with the recent analysis of novel Sec1p mutants, both support the idea that Sec1p is functional already before SNARE complex assembly (Wiederkehr *et al.*, 2004; Hashizume *et al.*, 2009). Several non-SNARE SM binding proteins interact directly or indirectly with Rab GTPases. This is the case, for example, for yeast Ivy1p and Vac1p and mammalian Mint proteins and granuphilin (Tall *et al.*, 1999; Coppola *et al.*, 2002; Lazar *et al.*, 2002; Teber *et al.*, 2005). Our results characterize Mso1p as a novel Rab GTPase binding protein in exocytic SNARE complex formation. The results suggest that Sec4p-Mso1p interaction may be initiated already in intracellular membranes prior to SNARE complex formation.

The molecular interactions revealed in this study add two previously uncharacterized (Sec1p tail-SNARE complexes and Mso1p-Sec4p) binding modes for central proteins in membrane fusion regulation. A challenge for future work will be to reveal the order of

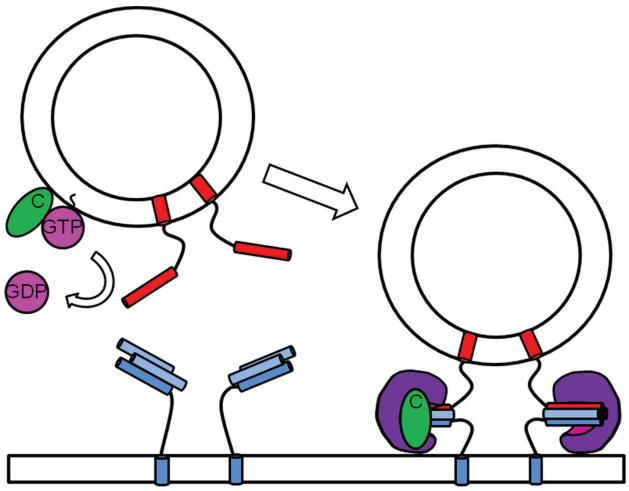

FIGURE 8: A schematic model for Mso1p and Sec1p C-terminal tail interactions during SNARE complex assembly. Mso1p is shown in green; the C marks the C terminus of Mso1p. Sec1p is shown in purple, and the area likely to be occupied by the Sec1p C-terminal tail (amino acids 658–724) is highlighted in magenta in Sec1p. Sec4p is shown in pink; the Q-SNAREs Sso1p and Sec9p in dark blue and light blue, respectively; and the R-SNARE Snc2p in red.

Name	Genotype	Source
H304	MAT**a** *leu2–3,112 ura3–52*	P. Novick
H1127	MATα *sec2–41 leu2–3,112 ura3–52*	P. Novick
H1152	MAT**a** *sso2–1 leu2–3,112 trp1–1 ura3–1 sso1::HIS3 ade2–1 his3–11,15 leu2–3,112 can1-100*	H. Ronne
H1910	MAT**a** *ura3 trp1 his3 6lexAop-LEU2*	E. Golemis
H2530	MAT**a**/MATα *leu2–3,112/leu2–3,112 ura3–52/ura3–52*	This study
H2598	MAT**a** *lys2 ura3 HO::hisG*	M. Knop
H2599	MATα *lys2 ura3 LEU2::hisG HO::LYS2*	M. Knop
H2657	MAT**a** *leu2–3,112 ura3–52 mso1::MSO1–3HA::kanMX*	Knop *et al.*, 2005
H2658	MAT**a** *leu2–3,112 ura3–52 mso1::hphMX*	Knop *et al.*, 2005
H2718	MAT**a** *DON1-GFP-kanMX4 SPO21 LEU2 lys2 ura3 KanMX mso1::hphMX4*	M. Knop
H2719	MATα *DON1-GFP-kanMX4 SPO21 leu2 ura3 LYS2 KanMX mso1::hphMX4*	M. Knop
H2728	MAT**a**/MATα *lys2/lys2 ura3/ura3 HO::hisG/HO::LYS2 LEU2/LEU2::hisG*	M. Knop
H3333	MAT**a** *ura3–52 lys2–801 trp1Δ63 his3Δ200 leu2Δ1*	M. Knop
H3366	MAT**a** *ura3–52 lys2–801 trp1Δ63 his3Δ200 leu2Δ1 SEC1::SEC1–3HA-kanMX*	Knop *et al.*, 2005
H3490	MAT**a**/MATα *DON1-GFP-kanMX4/DON1-GFP-kanMX4 SPO21/SPO21 LEU2/leu2 lys2/LYS2 ura3::YIpmso1PPP-URA3/ura3::YIpmso1PPP-URA3 KanMX* mso1::hphMX4/KanMx mso1::hphMX4	This study
H3658	MAT**a** *leu2–3,112 ura3–52 sec1::sec1(1–657)-hphMX*	This study
H3659	MAT**a** *leu2–3,112 ura3–52 mso1::MSO1–3HA::kanMX sec1::sec1(1–657)-hphMX*	This study
H3660	MAT**a** *lys2 ura3 HO::hisG sec1::sec1(1–657)-hphMX*	This study
H3661	MATα *lys2 ura3 LEU2::hisG HO::LYS2 sec1::sec1(1–657)-hphMX*	This study
H3662	MAT**a**/MATα *lys2/lys2 ura3/ura3 HO::hisG/HO::LYS2 LEU2/LEU2::hisG sec1::sec1(1–657)-hphMX/sec1::sec1(1–657)-hphMX*	This study
H3852	MAT**a** *ura3–52 lys2–801 trp1Δ63 his3Δ200 leu2Δ1 sec1::sec1(1–657)-3HA-hphMX*	This study

TABLE 1: Yeast strains.

the observed interactions in the regulation of SNARE complex formation.

MATERIALS AND METHODS

Strains

The yeast strains used are shown in Table 1. When not otherwise stated, yeast cells were grown essentially as described previously (Sherman, 1991). The *SEC1* C terminus was deleted after arginine 657 in H304, H2657, H2598, and H2599 to generate H3358, H3359, H3660, and H3661 by transformation with a PCR cassette that was generated using B2308 as the template (Janke *et al.*, 2004). The diploid H3662 expressing the C-terminal *sec1* mutant was generated by mating H3660 and H3661. To obtain strain H3852, *SEC1* was tagged with three HA-tags after arginine 657 in H3333 by a PCR cassette transformation using B2966 as template (Janke *et al.*, 2004). To obtain the diploid strain H3490, B2928 was integrated to the *ura3* locus of H2718 and H2719 followed by mating of the haploid strains.

Plasmids

Plasmids used are listed in Table 2. After PCR amplification with *Bam*HI or *Sal*I site containing oligonucleotides, the *SEC1(1–657)* fragment was cloned into B2930 by replacing the wt *SEC1* in B2930. To generate B3311, the *SEC1(1–657)* fragment was released with *Bam*HI/*Sal*I digestion from B3279 followed by ligation into B3021. For B3406 a *SEC1(658–724)* fragment was PCR amplified with *Bam*HI and *Sal*I sites followed by *Bam*HI/*Sal*I digestion and ligation into B3021. For B3405 the wt *SEC1* in B2930 was replaced by the *SEC1(658–724)* PCR product. For the generation of B3556, the *MSO1(1–188)* fragment was PCR amplified adding *Bgl*II and *Xho*I restriction sites, followed by *Bgl*II/*Xho*I digestion and ligation into B3031 linearized with *Bam*HI/*Xho*I. To generate B3316, wt *SEC4* was cut out with *Bam*HI and *Xho*I from B1326 and ligated into B3018. B3317, B3318, and B3319 were created by PCR amplification of *sec4(Q79L), SEC4(S34N)*, and *SEC4(N133I)* with *Bam*HI and *Xho*I sites digested with *Bam*HI/*Xho*I and ligation into B3018. To generate B3310, a *SSO1* fragment lacking the *trans*-membrane anchor coding sequence was released with *Eco*RI and *Xho*I from B3306 and cloned into B1231. For B3404, a *SEC1(658–724)* fragment was PCR amplified with *Eco*RI and *Sal*I sites and ligated into the *Eco*RI/*Xho*I cut B1226. For Sec1p C-terminal tail overexpression, a *SEC1(658–724)* fragment was cut out from B3404 with *Eco*RI and *Sal*I (the terminator was also released) and ligated into B2759 and B2757 to generate B3424 and B3484, respectively. For the production of the N-terminally His_6-tagged Sec1p tail in *Escherichia coli*, a *SEC1(658–724)* fragment was PCR amplified with *Eco*RI and *Sal*I sites, digested with *Eco*RI/*Sal*I and ligated into B3006 generating B3517. To obtain N-terminally MBP-tagged Sec1p tail, *SEC1(658–724)* was PCR amplified with *Nco*I and *Sal*I sites and ligated into B2876 to generate B3403. For the production of His_6-tagged Sso1p (B3445) and Snc2p (B3477), fragments encoding the cytosolic parts of these proteins were generated by PCR, trimmed with *Bam*HI/*Xho*I and *Hind*III/*Xho*I, respectively, and ligated into B3006. For B3448, a DNA fragment for *sec9(161–651)* was PCR amplified with *Bam*HI and *Xho*I sites followed by ligation into pYES2CT (Invitrogen, Carlsbad, CA). From there *sec9(161–651)* was cut out as an *Eco*RI/*Xho*I fragment and inserted into B3006 for the expression of a His_6-tagged Sec9p(161–651). To generate B2928, a stop codon was introduced by PCR after amino acid 188 in *MSO1* (B1885) followed by ligation into *Spe*I/*Xho*I cut B704. B3557 was generated by ligation of the *Eco*RI/*Xho*I cut PCR fragment for Sec4-CC (lacking the last two cysteins) into B1421 that had been cut with *Eco*RI and *Sal*I. All DNA constructs generated by PCR were verified by sequencing. The oligonucleotides used in this study are available upon request.

Immunoprecipitations

Immunoprecipitations were performed as described previously (Knop *et al.*, 2005). As a negative control, a lysate prepared from an isogenic untagged strain was used. For Western blot analysis,

Plasmid	Name	Type	Yeast promoter	Insert	Marker	Source
B371	YEp24H	*2μ*	-	-	*URA3*	E. Clark
B578	YCpSEC1-U	*2μ*	*Endogenous*	*SEC1 wt*	*URA3*	Aalto *et al.*, 1993
B698	pVT102U	*2μ*	*ADH1*	-	*URA3*	Vernet *et al.*, 1987
B704	pRS406	-	-	-	*URA3*	Sikorski and Hieter, 1989
B712	pRS426	*2μ*	-	-	*URA3*	Christianson *et al.*, 1992
B782	YEpSEC9-U	*2μ*	*Endogenous*	*SEC9 wt*	*URA3*	Brennwald *et al.*, 1994
B1226	PJG4–5	*2μ*	*GAL1*	-	*TRP1*	E. Golemis
B1227	pSH18–34	*2μ*	-	*8 ops-lacZ*	*URA3*	E. Golemis
B1228	pRFHM1	*2μ*	*ADH1*	*Bicoid*	*HIS3*	E. Golemis
B1229	pSH17–4	*2μ*	*ADH1*	*LexA-Gal4*	*HIS3*	E. Golemis
B1231	pEG202	*2μ*	*ADH1*	-	*HIS3*	E. Golemis
B1326	pGAT-SEC4	-	-	*SEC4*	-	Toikkanen *et al.*, 2003
B1421	pMAL-C2X	-	-	*MalE*	-	New England Biolabs
B1476	YEpSSO1U	*2μ*	*Endogenous*	*SSO1 wt*	*URA3*	Jäntti *et al.*, 2002
B1479	YEpSSO2U	*2μ*	*Endogenous*	*SSO2 wt*	*URA3*	Jäntti *et al.*, 2002
B1487	YEpSSO2-MA-bait	*2μ*	*ADH1*	*SSO2-MA*	*HIS3*	Brummer *et al.*, 2001
B1567	pUADH-mycSNC2	*CEN*	*ADH1*	*SNC2*	*URA3*	Lustgarten and Gerst, 1999
B1713	YEpSEC1-prey	*2μ*	*GAL1*	*SEC1 wt*	*TRP1*	Brummer *et al.*, 2001
B1719	YEpSEC1-bait	*2μ*	*ADH1*	*SEC1 wt*	*HIS3*	Brummer *et al.*, 2001
B1840	YEpMSO1(1–210)U	*2μ*	*ADH1*	*MSO1 wt*	*URA3*	Knop *et al.*, 2005
B1885	MSO1-Bluescript	-	-	*MSO1 wt*	-	
B2308	pFA6-hphNTI	-	-	-	-	Janke *et al.*, 2004
B2757	p424ADH	*2μ*	*ADH1*	-	*TRP1*	Mumberg *et al.*, 1995
B2759	p426ADH	*2μ*	*ADH1*	-	*URA3*	Mumberg *et al.*,1995
B2876	pETM-40	-	-	-	-	M. Knop
B2918	MSO1VC416ADH	*CEN*	*ADH1*	*MSO1 wt*	*URA3*	Weber *et al.*, 2010
B2928	YIpMSO1(1–188)-U	-	*Endogenous*	*MSO1(1–188)*	*URA3*	This study
B2930	YCpSEC1-VN-L	*CEN*	*ADH1*	*SEC1 wt*	*LEU2*	Weber *et al.*, 2010
B2966	pYM24	-	-	-	-	Janke *et al.*, 2004
B3006	pRSFDuet-1	-	-	-	-	Novagen
B3018	N-YN425ADH	*2μ*	*ADH1*	*YFP N-term*	*LEU2*	Skarp *et al.*, 2008
B3020	N-YC426ADH	*2μ*	*ADH1*	*YFP C-term*	*URA3*	Skarp *et al.*, 2008
B3021	C-YC426ADH	*2μ*	*ADH1*	*YFP C-term*	*URA3*	Skarp *et al.*, 2008
B3022	pFA6-natNT2	-	-	-	-	Janke *et al.*, 2004
B3031	p416 MET YC-CDC42	*CEN*	*MET25*	*CDC42*	*URA3*	Cole *et al.*, 2007
B3043	YCpYC-MSO1(136–210)-U	*CEN*	*MET25*	*MSO1(136–210)*	*URA3*	Weber *et al.*, 2010
B3044	YCpYC-MSO1-U	*CEN*	*MET25*	*MSO1 wt*	*URA3*	Weber *et al.*, 2010
B3276	YEpSSO2-MA-prey	*2μ*	*GAL1*	*SSO2-MA*	*TRP1*	Weber *et al.*, 2010
B3279	YCpSEC1(1–657)-VN-L	*CEN*	*ADH1*	*sec1(1–657)*	*LEU2*	This study
B3306	YEpSSO1-MA-prey	*2μ*	*GAL1*	*SSO1-MA*	*TRP1*	Weber *et al.*, 2010
B3307	YEpYN-SSO1-L	*2μ*	*ADH1*	*SSO1*	*LEU2*	Weber *et al.*, 2010
B3308	YEpSEC1-YC-U	*2μ*	*ADH1*	*SEC1(wt)*	*URA3*	Weber *et al.*, 2010
B3309	YEpYN-SSO2-L	*2μ*	*ADH1*	*SSO2*	*LEU2*	Weber *et al.*, 2010
B3310	YEpSSO1-MA-bait	*2μ*	*ADH1*	*SSO1-MA*	*HIS3*	This study
B3311	YEpsec1(1–657)-YC-U	*2μ*	*ADH1*	*sec1(1–657)*	*URA3*	This study
B3316	YEpYN-SEC4-L	*2μ*	*ADH1*	*SEC4(wt)*	*LEU2*	This study
B3317	YEpYN-SEC4(Q79L)-L	*2μ*	*ADH1*	*SEC4(Q79L)*	*LEU2*	This study
B3318	YEpYN-SEC4(N34)-L	*2μ*	*ADH1*	*SEC4(S34N)*	*LEU2*	This study
B3319	YEpYN-SEC4(I133)-L	*2μ*	*ADH1*	*SEC4(N133I)*	*LEU2*	This study
B3354	YCpYC-MSO1(1–135)-U	*CEN*	*MET25*	*MSO1(1–135)*	*URA3*	Weber *et al.*, 2010
B3403	SEC1(658–724)pETM-40	-	-	*SEC1(658–724)*	-	This study
B3404	YEpSEC1(658–724)-prey	*2μ*	*GAL1*	*SEC1(658–724)*	*TRP1*	This study
B3405	YCpSEC1(658–724)-VN-L	*CEN*	*ADH1*	*SEC1(658–724)*	*LEU2*	This study
B3406	YCpsec1(658–724)-YC-U	*2μ*	*ADH1*	*SEC1(658–724)*	*URA3*	This study
B3424	YEpSEC1(658–724)-U	*2μ*	*ADH1*	*SEC1(658–724)*	*URA3*	This study
B3445	SSO1-MA-pRSFDuet-1	-	-	*SSO1-MA*	-	This study
B3448	SEC9(161–651)-pRSDuet-1	-	-	*SEC9(161–651)*	-	This study
B3477	SNC2-MA-pRSDuet-1	-	-	*SNC2-MA*	-	This study
B3484	YEpSEC1(658–724)-T	*2μ*	*ADH1*	*SEC1(658–724)*	*TRP1*	This study
B3517	SEC1(658–724)pRSFDuet-1	-	-	*SEC1(658–724)*	-	This study
B3556	YCpYC-MSO1(1–188)-U	*CEN*	*MET25*	*MSO1(1–188)*	*URA3*	This study
B3557	SEC4-CC pMAL-C2X	-	-	*SEC4-CC*	-	This study

TABLE 2: Plasmids.

proteins were transferred onto nitrocellulose membranes. Bound antibodies were visualized with the ECL detection system (Pierce, Rockford, IL). Each immunoprecipitation was performed at least three times. Quantifications were performed using Bio-Rad (Hercules, CA) Quantity One software and normalized for the amount of immunoprecipitated Mso1p-HA or myc-Snc2p.

Membrane fractionations

Cells were grown and lysed in the same way as for immunoprecipitations. After lysis, the lysates were centrifuged at 10,000 × *g* for 10 min at 4°C. The obtained supernatant (S2) was further centrifuged at 100,000 × *g* for 1 h at 4°C to obtain supernatant (S3) and pellet (P3), which was resuspended to the same volume as S3. Identical volumes of these fractions were subjected to SDS–PAGE and Western blotting. The Western results were quantified using Bio-Rad Quantity One software.

Secretion assays

The intracellular accumulation of Bgl2p was measured essentially as described previously (Harsay and Schekman, 2007). In brief, *SEC1* wt (H2657) and *sec1(1–657)* mutant (H3659) stains were grown to OD 0.3–0.6, split to two identical cultures, and shifted to 30°C or 37°C. Cells were collected at indicated time points, and cell lysates were generated. Accumulated Bgl2p was detected with anti-Bgl2p antibody by Western blotting. Quantification of Hsp150 secretion was carried out from similarly treated cells as previously described (Davydenko *et al.*, 2005).

Antibodies

The HA (12CA5) and the myc-tag antibodies (9E10) were purchased from Roche, Basel, Switzerland. Anti-Sec1p antibodies used were the anti-Sec1p (#57) (Scott *et al.*, 2004) from James McNew (Rice University, Houston, TX). Anti-Sec9p-CT antibodies (Brennwald *et al.*, 1994) were obtained from Patrick Brennwald (University of North Carolina at Chapel Hill), anti-Bgl2p antibodies (Harsay and Schekman, 2007) were obtained from Edina Harsay (University of Kansas, Lawrence), anti-Hsp150 antibody (Russo *et al.*, 1992) was obtained from Marja Makarow (Institute of Biotechnology, University of Helsinki, Finland), and anti-Snc1p and Snc2p antibodies were obtained from Michael Knop (European Molecular Biology Laboratory [EMBL], Heidelberg, Germany). Anti-Sec4p (R232), Sec15p (R233), Sso1/2p (K8), Sso1p (K6916), Sso2p (K6906), and Mso1p (R285) have been described previously (Aalto *et al.*, 1997; Jäntti *et al.*, 2002; Toikkanen *et al.*, 2003; Knop *et al.*, 2005).

Fluorescence microscopy

Cells were grown to OD_{600} 0.8–1 at the permissive temperature. In the case of temperature-sensitive strains, cells were shifted to the restrictive temperature for 1 h prior to microscopy. Cells were observed using an Olympus PROVIS microscope with a plan apo 60×/1,40 Oil ph3 (Japan) objective and bright field and appropriate filters. The analySIS Image Processing software (Olympus Soft Imaging Solutions GmbH, Münster, Germany) was used for recording the images. The exposure time for the BiFC was 2–5 s for Mso1p-Sec1p, Mso1p-Sso1/2p, Sec9p-Sec4p, and Mso1p-Sec4p interaction and 1–2 s for Sso1/2p-Sec1p interaction. Image panels were prepared using Adobe Photoshop7 software. For quantification of the signal intensity, the original images were used. The images ware taken using the same microscope and the same exposure time. No image manipulations were used before the quantifications. Images with uneven lighting were omitted from the analysis. The interaction intensities were quantified by measuring the mean gray value of random points on the plasma membrane or in the cytosol using ImageJ 1.42. For the Sso1/2p-Sec1p interactions, the signal was measured at the mother plasma membrane opposite the bud. For the Mso1p-Sec1p interaction, the signal was measured in the bud tip and in the mother cell cytosol. For the Mso1p-Sso1/2p interaction, the signal intensities were measured at the bud tip of the daughter cell plasma membrane and opposite the bud at the mother cell plasma membrane in the same cell. The obtained intensities were averaged to get a mean total signal intensity value. For each condition, the signal in at least 50 cells was quantified. The background fluorescence was randomly measured at 10 points per condition in all images and subsequently subtracted from the obtained measurements. Typically, for BiFC experiments no signal was observed in ~40% of the cells. These cells were omitted from the analysis of the signal distribution.

Yeast two-hybrid assay

The yeast two-hybrid assay was performed essentially as described previously (Golemis *et al.*, 1998; Weber *et al.*, 2010). The EGY48 (H1910) strain was used for the assay. The plasmids B1227 (pSH18–34), B1228 (pRFHM1), and B1229 (pSH17–4) were used as positive and negative controls. Four individual colonies of each transformation were examined for growth on SC-ura-leu-his-trp + 1% raffinose + 2% galactose.

Recombinant protein purification

Sec1p(658–724) was produced as fusion protein with N-terminal MBP. A cell pellet from a 500-ml culture was resuspended in 10 ml of buffer 150 (20 mM Tris–HCl, pH 8, 150 mM NaCl, 5 mM $MgCl_2$) and lysed on ice by sonication (four times for 30 s with 30-s intervals). Cell debris was removed by centrifugation at 10,000 × *g* for 10 min at 4°C. The supernatant was mixed with 500 µl of amylose resin, and the MBP-Sec1p(658–724) was allowed to bind at 4°C for 1 h. The resin was collected by centrifugation at 10,000 × *g* for 5 s, washed three times with 10 ml of buffer 500 (20 mM Tris–HCl, pH 8, 500 mM NaCl, 5 mM $MgCl_2$) and three times with 10 ml of 50 mM HEPES, pH 7.2. The resin-bound MBP-Sec1p(658–724) was stored in 50 mM HEPES, pH 7.2 at 4°C as a 50% slurry. MBP was produced and purified in the same way. MBP-Sec4p-CC and MBP were produced in the same way as just described, except that the storage buffer for the proteins was 25 mM HEPES, pH 7.2, 150 mM KCl. Sec1p(658–724), the cytosolic parts of Sso1p (amino acids 1–265) and Snc2p (amino acids 1–93), and Sec9p (amino acids 161–651) were produced in *E. coli* as fusion protein with an N-terminal His_6-tag and purified using standard Ni-NTA (nickel–nitriloacetic acid) purification methods.

In vitro pull-down assays

Binary complexes (Sso1p-Sec9p) and tertiary complexes (Sso1p-Sec9p-Snc2p) were preformed by mixing equal amounts of the proteins (100 µM each) in a total volume of 100 µl of binding buffer (50 mM HEPES, pH 7.2) and incubation at 16°C overnight. For the pull-down experiments, 4 µM MBP-Sec1p(658–724) or MBP bound to amylose resin was combined with 3 or 10 µM Sso1p, binary complexes, or tertiary complexes and incubated at room temperature in a total volume of 100 µl of the binding buffer for 1 h with gentle mixing. After the incubation, the resin was washed three times with 1 ml of the binding buffer. The bound proteins were released into 50 µl of 1× LSB (Laemmli sample buffer) by heating for 5 min at 95°C and subjected to SDS–PAGE. Quantifications were performed using Bio-Rad Quantity One software and normalized for the amount of MBP or MBP-Sec1p(658–724).

For in vitro pull-down experiments between Mso1p and Sec4p-CC, 4 µM MBP-Sec4p-CC or MBP alone immobilized on amylose resin was used. These proteins were combined with 8 µM

N-terminally tagged Mso1p or the tag alone (unpublished data), 10 μM γGTP, and 0.5% Nonidet P-40 (NP-40). The mixtures were incubated at room temperature in a total volume of 100 μl of the binding buffer (25 mM HEPES, pH 7.2, 150 mM KCl) for 2 h with gentle mixing. After the incubation, the resin was washed three times with 1 ml of the binding buffer. The bound proteins were released into 50 μl of 1× LSB by heating for 5 min at 95°C and subjected to SDS–PAGE and Western blotting with tag-specific antibodies.

In vitro gel mobility shift assay

Samples containing Snc2p, Sso1p, Sec9p (30 μM each), and His_6-Sec1p(658–725) (0, 15, 30, and 60 μM) were incubated at room temperature or 4°C in the binding buffer (20 mM Tris-HCl, pH 8, 200 mM NaCl) for 1, 2, or 24 h. The complexes were resolved in an 8% native gel run toward the positively charged electrode and stained with Coomassie Brilliant Blue.

Secondary structure prediction

Secondary structure prediction was performed using the PSIPRED Protein Structure Prediction Server (http://128.16.10.201/psipred/; Jones, 1999; Bryson *et al.*, 2005).

ACKNOWLEDGMENTS

Dennis Bamford, Pat Brennwald, Jeffrey Gerst, Wei Guo, Edina Harsay, Marko Hyvönen, Michael Knop, Marja Makarow, James McNew, Mary Munson, Peter Novick, and Johan Peranen are acknowledged for generously providing us with strains, plasmids, and/or antibodies. Members of the Jäntti lab are thanked for discussions, ideas, and comments on the manuscript. Anna-Liisa Nyfors is thanked for excellent technical assistance. Maria Aatonen is acknowledged for excellent cooperation in the Biacore analysis. This work was financially supported by the Academy of Finland (Grants 124249 and 133552 to J.J. and 123733 to N.A.), the Magnus Ehrnrooth Foundation (J.J.), and the Institute of Biotechnology (J.J.). M.W. was supported by the Viikki Graduate School in Biosciences and the Alfred Kordelin Foundation.

REFERENCES

Aalto MK, Jantti J, Ostling J, Keranen S, Ronne H (1997). Mso1p: a yeast protein that functions in secretion and interacts physically and genetically with Sec1p. Proc Natl Acad Sci USA 94, 7331–7336.

Aalto MK, Ronne H, Keränen S (1993). Yeast syntaxins Sso1p and Sso2p belong to a family of related membrane proteins that function in vesicular transport. EMBO J 12, 4095–4104.

Albert S, Gallwitz D (1999). Two new members of a family of Ypt/Rab GTPase activating proteins—promiscuity of substrate recognition. J Biol Chem 274, 33186–33189.

Albert S, Gallwitz D (2000). Msb4p, a protein involved in Cdc42p-dependent organization of the actin cytoskeleton, is a Ypt/Rab-specific GAP. Biol Chem 381, 453–456.

Arac D, Dulubova I, Pei JM, Huryeva I, Grishin NV, Rizo J (2005). Three-dimensional structure of the rSly1 N-terminal domain reveals a conformational change induced by binding to syntaxin 5. J Mol Biol 346, 589–601.

Armstrong J (2000). How do Rab proteins function in membrane traffic? Int J Biochem Cell Biol 32, 303–307.

Bracher A, Weissenhorn W (2002). Structural basis for the Golgi membrane recruitment of Sly1p by Sed5p. EMBO J 21, 6114–6124.

Brennwald P, Kearns B, Champion K, Keranen S, Bankaitis V, Novick P (1994). Sec9 is a SNAP-25-like component of a yeast SNARE complex that may be the effector of Sec4 function in exocytosis. Cell 79, 245–258.

Brummer MH, Kivinen KJ, Jäntti J, Toikkanen J, Söderlund H, Keränen S (2001). Characterization of the sec1-1 and sec1-11 mutations. Yeast 18, 1525–1536.

Bryson K, McGuffin LJ, Marsden RL, Ward JJ, Sodhi JS, Jones DT (2005). Protein structure prediction servers at University College London. Nucleic Acids Res 33, W36–W38.

Carpp LN, Ciufo LF, Shanks SG, Boyd A, Bryant NJ (2006). The Sec1p/Munc18 protein Vps45p binds its cognate SNARE proteins via two distinct modes. J Cell Biol 173, 927–936.

Carr CM, Grote E, Munson M, Hughson FM, Novick PJ (1999). Sec1p binds to SNARE complexes and concentrates at sites of secretion. J Cell Biol 146, 333–344.

Carr CM, Rizo J (2010). At the junction of SNARE and SM protein function. Curr Opin Cell Biol 22, 488–495.

Castillo-Flores A, Weinberger A, Robinson M, Gerst JE, (2005). Mso1 is a novel component of the yeast exocytic SNARE complex. J Biol Chem 280, 34033–34041.

Christianson TW, Sikorski RS, Dante M, Shero JH, Hieter P (1992). Multifunctional yeast high-copy-number shuttle vectors. Gene 110, 119–122.

Cole KC, McLaughlin HW, Johnson DI (2007). Use of bimolecular fluorescence complementation to study in vivo interactions between Cdc42p and Rdi1p of Saccharomyces cerevisiae. Eukaryotic Cell 6, 378–387.

Collins RN, Brennwald P, Garrett M, Lauring A, Novick P (1997). Interactions of nucleotide release factor Dss4p with Sec4p in the post-Golgi secretory pathway of yeast. J Biol Chem 272, 18281–18289.

Coppola T, Frantz C, Perret-Menoud V, Gattesco S, Hirling H, Regazzi R (2002). Pancreatic beta-cell protein granuphilin binds Rab3 and Munc-18 and controls exocytosis. Mol Biol Cell 13, 1906–1915.

Davydenko SG, Feng D, Jantti J, Keranen S (2005). Characterization of GPI14/YJR013w mutation that induces the cell wall integrity signalling pathway and results in increased protein production in Saccharomyces cerevisiae. Yeast 22, 993–1009.

Deak F, Xu Y, Chang WP, Dulubova I, Khvotchev M, Liu XR, Sudhof TC, Rizo J (2009). Munc18–1 binding to the neuronal SNARE complex controls synaptic vesicle priming. J Cell Biol 184, 751–764.

Du LL, Collins RN, Novick PJ (1998). Identification of a Sec4p GTPase-activating protein (GAP) as a novel member of a Rab GAP family. J Biol Chem 273, 3253–3256.

Dulubova I, Yamaguchi T, Gao Y, Min SW, Huryeva I, Sudhof TC, Rizo J (2002). How Tlg2p/syntaxin 16 "snares" Vps45. EMBO J 21, 3620–3631.

Furgason MLM, Macdonald C, Shanks SG, Ryder SP, Bryant NJ, Munson M (2009). The N-terminal peptide of the syntaxin Tlg2p modulates binding of its closed conformation to Vps45p. Proc Natl Acad Sci USA 106, 14303–14308.

Gallwitz D, Jahn R (2003). The riddle of the Sec1/Munc-18 proteins—new twists added to their interactions with SNAREs. Trends Biochem Sci 28, 113–116.

Golemis EA, Serebriiskii I, Finlay RL, Kolonin MG, Gyuris J, Brent R (1998). Interaction trap/two-hybrid system to identify interacting proteins. In: Current Protocols in Protein Science, ed. FM Ausubel, New York: Wiley Interscience.

Goud B, Salminen A, Walworth NC, Novick PJ (1988). A GTP-binding protein required for secretion rapidly associates with secretory vesicles and the plasma membrane in yeast. Cell 53, 753–768.

Guo W, Roth D, Walch-Solimena C, Novick P (1999). The exocyst is an effector for Sec4p, targeting secretory vesicles to sites of exocytosis. EMBO J 18, 1071–1080.

Guo W, Sacher M, Barrowman J, Ferro-Novick S, Novick P (2000). Protein complexes in transport vesicle targeting. Trends Cell Biol 10, 251–255.

Harsay E, Bretscher A, (1995). Parallel secretory pathways to the cell surface in yeast. J Cell Biol 131, 297–310.

Harsay E, Schekman R, (2007). Avl9p, a member of a novel protein superfamily, functions in the late secretory pathway. Mol Biol Cell 18, 1203–1219.

Hashizume K, Cheng YS, Hutton JL, Chiu CH, Carr CM (2009). Yeast Sec1p functions before and after vesicle docking. Mol Biol Cell 20, 4673–4685.

He B, Guo W (2009). The exocyst complex in polarized exocytosis. Curr Opin Cell Biol 21, 537–542.

Hu SH, Latham CF, Gee CL, James DE, Martin JL (2007). Structure of the Munc18c/Syntaxin4 N-peptide complex defines universal features of the N-peptide binding mode of Sec1/Munc18 proteins. Proc Natl Acad Sci USA 104, 8773–8778.

Jahn R, Scheller RH (2006). SNAREs—engines for membrane fusion. Nat Rev Mol Cell Biol 7, 631–643.

Janke C *et al.* (2004). A versatile toolbox for PCR-based tagging of yeast genes: new fluorescent proteins, more markers and promoter substitution cassettes. Yeast 21, 947–962.

Jäntti J, Aalto MK, Oyen M, Sundqvist L, Keranen S, Ronne H (2002). Characterization of temperature-sensitive mutations in the yeast syntaxin 1 homologues Sso1p and Sso2p, and evidence of a distinct function for Sso1p in sporulation. J Cell Sci 115, 409–420.

Jones DT (1999). Protein secondary structure prediction based on position-specific scoring matrices. J Mol Biol 292, 195–202.
Kauppi M, Jäntti J, Olkkonen VM (2004). The function of Sec1/Munc18 proteins-solution of the mystery in sight? In: Regulatory Mechanisms of Intracellular Membrane Transport, ed. S Keränen and J Jäntti, Berlin: Springer-Verlag, 115–143.
Knop M, Miller KJ, Mazza M, Feng DJ, Weber M, Keranen S, Jantti J (2005). Molecular interactions position Mso1p, a novel PTB domain homologue, in the interface of the exocyst complex and the exocytic SNARE machinery in yeast. Mol Biol Cell 16, 4543–4556.
Latham CF *et al*. (2006). Molecular dissection of the Munc18c/syntaxin4 interaction: implications for regulation of membrane trafficking. Traffic 7, 1408–1419.
Lazar T, Scheglmann D, Gallwitz D (2002). A novel phospholipid-binding protein from the yeast Saccharomyces cerevisiae with dual binding specificities for the transport GTPase Ypt7p and the Sec 1-related Vps33p. Eur J Cell Biol 81, 635–646.
Lustgarten V, Gerst JE (1999). Yeast VSM1 encodes a v-SNARE binding protein that may act as a negative regulator of constitutive exocytosis. Mol Cell Biol 19, 4480–4494.
Misura KM, Scheller RH, Weis WI (2000). Three-dimensional structure of the neuronal-Sec1-syntaxin 1a complex. Nature 404, 355–362.
Mizuno-Yamasaki E, Medkova M, Coleman J, Novick P (2010). Phosphatidylinositol 4-phosphate controls both membrane recruitment and a regulatory switch of the Rab GEF Sec2p. Dev Cell 18, 828–840.
Mumberg D, Muller R, Funk M (1995). Yeast vectors for the controlled expression of heterologous proteins in different genetic backgrounds. Gene 156, 119–122.
Munson M, Bryant NJ (2009). A role for the syntaxin N-terminus. Biochem J 418, e1–e3.
Munson M, Novick P (2006). The exocyst defrocked, a framework of rods revealed. Nat Struct Mol Biol 13, 577–581.
Neiman AM (1998). Prospore membrane formation defines a developmentally regulated branch of the secretory pathway in yeast. J Cell Biol 140, 29–37.
Neiman AM (2005). Ascospore formation in the yeast Saccharomyces cerevisiae. Microbiol Mol Biol Rev 69, 565–584.
Novick P, Guo W (2002). Ras family therapy: Rab, Rho and Rai talk to the exocyst. Trends Cell Biol 12, 247–249.
Nunes Bastos R (2008). Functional dissection of alternative secretory pathways in the yeast S. cerevisiae. PhD Thesis. Dissertationes bioscientiarum molecularium Universitatis Helsingiensis in Viikki. ISBN 978–952-10–4736-7.
Peng RW, Gallwitz D (2002). Sly1 protein bound to Golgi syntaxin Sed5p allows assembly and contributes to specificity of SNARE fusion complexes. J Cell Biol 157, 645–655.
Russo P, Kalkkinen N, Sareneva H, Paakkola J, Makarow M (1992). A heat shock gene from Saccharomyces cerevisiae encoding a secretory glycoprotein. Proc Natl Acad Sci USA 89, 3671–3675.
Scott BL, Van Komen JS, Irshad H, Liu S, Wilson KA, McNew JA (2004). Sec1p directly stimulates SNARE-mediated membrane fusion in vitro. J Cell Biol 167, 75–85.
Shen JS, Tareste DC, Paumet F, Rothman JE, Melia TJ (2007). Selective activation of cognate SNAREpins by Sec1/Munc18 proteins. Cell 128, 183–195.
Sherman F (1991). Getting started with yeast. In: Guide to Yeast Genetics and Molecular Biology, ed. C Guthrie and GR Fink, San Diego, CA: Academic Press, 3–21.
Sikorski RS, Hieter P (1989). A system of shuttle vectors and yeast host strains designed for efficient manipulation of DNA in Saccharomyces cerevisiae. Genetics 122, 19–27.
Skarp KP, Zhao X, Weber M, Jantti J (2008). Use of bimolecular fluorescence complementation in yeast Saccharomyces cerevisiae. Methods Mol Biol 457, 165–175.
Strop P, Kaiser SE, Vrljic M, Brunger AT (2008). The structure of the yeast plasma membrane SNARE complex reveals destabilizing water-filled cavities. J Biol Chem 283, 1113–1119.
Tall GG, Hama H, Dewald DB, Horazdovsky BF (1999). The phosphatidylinositol 3-phosphate binding protein Vac1p interacts with a Rab GTPase and a Sec1p homologue to facilitate vesicle-mediated vacuolar protein sorting. Mol Biol Cell 10, 1873–1889.
Tarassov K *et al*. (2008). An in vivo map of the yeast protein interactome. Science 320, 1465–1470.
Teber I, Nagano F, Kremerskothen J, Bilbilis K, Goud B, Barnekow A (2005). Rab6 interacts with the mint3 adaptor protein. Biol Chem 386, 671–677.
Togneri J, Cheng YS, Munson M, Hughson FM, Carr CM (2006). Specific SNARE complex binding mode of the Sec1/Munc-18 protein, Sec1p. Proc Natl Acad Sci USA 103, 17730–17735.
Toikkanen JH, Miller KJ, Soderlund H, Jantti J, Keranen S (2003). The beta subunit of the Sec61p endoplasmic reticulum translocon interacts with the exocyst complex in Saccharomyces cerevisiae. J Biol Chem 278, 20946–20953.
Toonen RF, Verhage M (2003). Vesicle trafficking: pleasure and pain from SM genes. Trends Cell Biol 13, 177–186.
Toonen RFG, Verhage M (2007). Munc18 = 1 in secretion: lonely Munc joins SNARE team and takes control. Trends Neurosci 30, 564–572.
Vernet T, Dignard D, Thomas DY (1987). A family of yeast expression vectors containing the phage f1 intergenic region. Gene 52, 225–233.
Walch-Solimena C, Collins RN, Novick PJ (1997). Sec2p mediates nucleotide exchange on Sec4p and is involved in polarized delivery of post-Golgi vesicles. J Cell Biol 137, 1495–1509.
Walworth NC, Brennwald P, Kabcenell AK, Garrett M, Novick P (1992). Hydrolysis of Gtp by Sec4 protein plays an important role in vesicular transport and is stimulated by a Gtpase-activating protein in Saccharomyces cerevisiae. Mol Cell Biol 12, 2017–2028.
Weber M, Chernov K, Turakainen H, Wohlfahrt G, Pajunen M, Savilahti H, Jantti J (2010). Mso1p regulates membrane fusion through interactions with the putative N-peptide-binding area in Sec1p domain 1. Mol Biol Cell 21, 1362–1374.
Wiederkehr A, De Craene JO, Ferro-Novick S, Novick P (2004). Functional specialization within a vesicle tethering complex: bypass of a subset of exocyst deletion mutants by Sec1p or Sec4p. J Cell Biol 167, 875–887.
Xu Y, Su LJ, Rizo J (2010). Binding of Munc18–1 to synaptobrevin and to the SNARE four-helix bundle. Biochemistry 49, 1568–1576.
Yamaguchi T, Dulubova I, Min SW, Chen XH, Rizo J, Sudhof TC (2002). Sly1 binds to Golgi and ER syntaxins via a conserved N-terminal peptide motif. Dev Cell 2, 295–305.